Nucleon Form Factors and Evidence for the Validity of Quantum Electrodynamics at Small Distances*

F. M. Pipkin

Harvard University,
Cambridge, Massachusetts

Introduction

In this paper I shall attempt to review the present experimental status of the general subject of electromagnetic interactions. The electromagnetic interactions can be divided into two main categories - interactions that include the strongly interacting particles, and interactions that deal only with photons and leptons. In the first category we come into contact with the whole field of strong interactions and the hope that the well-understood electromagnetic interaction can be used to probe the structure of the elementary particles. The second category comprises what is normally referred to as quantum electrodynamics. Quantum electrodynamics is the only really successful field theory. It has had amazing success in predicting the details of the low momentum transfer interactions of photons, muons, and electrons. The manner in which electrodynamics has been reformulated to overcome the self-energy infinities leads one to distrust its predictions at higher energy, and to hope that future experiments will suggest how to reformulate the theory so that it can predict the mass and charge of the leptons. At the present time both of these fields are particularly interesting. Not only do we now have many excellent electron-scattering experiments from which we can determine the structure of the nucleons, but soon we will have information on the form factors in the time-like region from proton-antiproton annihilation experiments and possible even from electron-positron storage rings. As a result of the discovery of the CP violation in the decay of the K_2^0 meson, charge conjugation invariance in the electromagnetic interaction of the strongly interacting particles has been questioned. Doubt has been cast on the use of the principle of the minimum electromagnetic coupling to determine the interaction of the elementary particles and the electromagnetic field. We now have several new tests of quantum electrodynamics at high momentum transfer. One experiment has even been reported in which there seems to be a deviation from the theory. In the first section of this review I shall discuss the present state of our knowledge of the nucleon form factors; in the second section I shall discuss the present evidence for the validity of quantum electrodynamics.

Nucleon Form Factors

The neutron and proton electromagnetic form factors furnish information on the charge structure of the nucleons and the currents which contribute to their anomalous magnetic moments. There are three independent sources of information concerning these form factors - electron scattering, proton-antiproton annihilation into electron-positron pairs, and electron-positron annihilation into proton-antiproton pairs. Electron scattering experiments measure the form factors for space-like momentum transfers; the annihilation experiments measure the form factors for time-like momentum transfers. The results of these two kinds of experiments can be related through dispersion relations which make use of the analytic structure of the form factors. Most of the present knowledge of the form factors comes from electron scattering experiments; experiments on the annihilation of proton-antiproton pairs into lepton pairs are now underway at Brookhaven and CERN; there are at present no operating storage rings with a sufficiently large energy to study electron-positron annihilation into proton-antiproton pairs. In this section the present status of our knowledge of these form factors will be reviewed.[1]

It is convenient to introduce the nucleon form factors through the expression

$$\langle p_f | j_\mu(o) | p_i \rangle = \frac{1}{\sqrt{4E_iE_f}} \left(\bar{U}_{pf} | F_1(q^2)\gamma_\mu + i\kappa F_2(q^2)\, \sigma_{\mu\nu} q_\nu | U_{pi} \right) \tag{1}$$

*Work supported by US Atomic Energy Commission

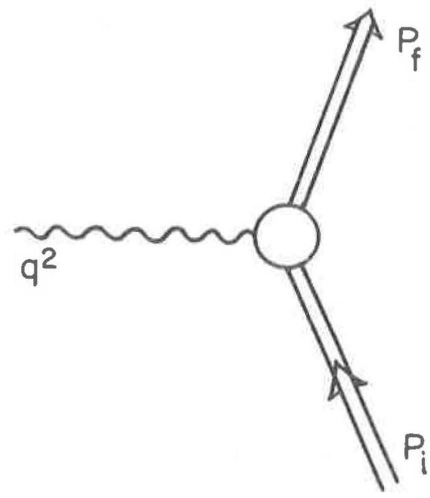

Figure 1 General vertex for the interaction of a nucleon and the electro-magnetic field.

This is the most general form consistent with Lorentz invariance and gauge invariance for the nucleon-photon interaction vertex shown in Figure 1. The initial and final nucleons are assumed to be on the mass shell and satisfy the free Dirac equation. The momentum transfer q^2 is given by[2]

$$q^2 = (p_f - p_i)^2, \tag{2}$$

and κ is the anomalous magnetic moment of the nucleon in units of the Bohr magneton. $F_1(q^2)$ is the Dirac form factor and $F_2(q^2)$ is the Pauli form factor. The F_1 and F_2 are normalized such that $F_1(0) = F_2(0) = 1$. This form of the matrix element is useful for calculating the cross section for electron-proton scattering and through electron-scattering experiments determines the form factors for space-like ($q^2 < 0$) momentum transfers. The general form for the amplitude to create a nucleon-antinucleon pair from a virtual photon can be used to define the form factors in the time-like region. The most general form for this amplitude is

$$<\bar{p}\, p'|j_\mu(o)|0> = \frac{1}{\sqrt{4\bar{E}E}} \; (U_{p'}|F_1(q^2)\,\gamma_\mu + i\,\kappa\, F_2(q^2)\sigma_{\mu\nu}\, q_\nu|V_{\bar{p}}). \tag{3}$$

It can be shown that this definition of F_1 and F_2 coincides with the analytic continuation of 1 when the form factors are treated as functions of the complex variable Z where $Z = q^2$.

In dealing with the form factors it is convenient to introduce two combinations of F_1 and F_2. These combinations are

$$G_E(q^2) = F_1(q^2) - \tau\,\kappa\, F_2(q^2),$$

and (4)

$$G_M(q^2) = F_1(q^2) + \kappa\, F_2(q^2).$$

Here $\tau = -q^2/4M^2$ and M is the mass of the proton. In terms of G_E and G_M, F_1 and F_2 are given by the equations

$$F_1(q^2) = \frac{G_E + \tau\, G_M}{1+\tau},$$

(5)

$$\kappa\, F_2(q^2) = \frac{G_M - G_E}{1+\tau}.$$

It is convenient to distinguish the proton and neutron form factors by using a subscript p or n. At $q^2 = 0$, G_E and G_M give the nucleon charge and magnetic moment in units of the electron charge and the nuclear magneton. That is

$$G_{E_p}(o) = 1 \quad ; \qquad G_{E_n}(o) = 0$$

(6)

$$G_{M_p}(o) = 2.793 \quad ; \qquad G_{M_n}(o) = -1.913.$$

It is useful to introduce the isotopic vector and the isotopic scalar form factors through the equations

$$\begin{aligned} G_{E_v} &= \frac{1}{2}(G_{E_p} - G_{E_n}) \;, \\ G_{E_s} &= \frac{1}{2}(G_{E_p} + G_{E_n}) \;, \\ G_{M_v} &= \frac{1}{2}(G_{M_p} - G_{M_n}) \;, \\ G_{M_s} &= \frac{1}{2}(G_{M_p} + G_{M_n}) \;. \end{aligned} \tag{7}$$

It is not clear which is the more fundamental set of form factors, the F's or the G's. The G's are simpler to determine experimentally since they enter the experimental cross sections for electron scattering and annihilation experiments only in terms of their squares. Sachs[3] has shown that if for electron scattering one goes to the coordinate system (the Breit frame) in which there is no energy transfer ($(q_0)_B = 0$), $G_E(q^2)$ and $G_M(q^2)$ are the fourier transforms of the nucleon charge and magnetic moment distributions. F_1 and F_2 appear to have a simpler analytic structure and no singularities.[4] In view of equations 5, this implies that for

$$\begin{aligned} q^2 &= 4M^2, \\ G_E(4M^2) &= G_M(4M^2). \end{aligned} \tag{8}$$

Otherwise these would be a pole in F_1 and F_2. The point $q^2 = 4M^2$ corresponds to the threshold for electron-positron annihilation into proton-antiproton pairs; the relationship 8 is necessary for the angular distribution of the proton-antiproton pairs at threshold to be isotropic. There also exists a simple experimental relationship between $G_{E\,p}$, $G_{M\,p}$ and $G_{M\,n}$ which may imply that they are more fundamental.

In terms of G_E and G_M the Rosenbluth cross section for electron proton scattering in the laboratory coordinate system is

$$\frac{d\sigma}{d\Omega} = \sigma_{NS}\left[\frac{G_E^2 + \tau G_M^2}{1+\tau} + 2\tau G_M^2 \tan^2\theta/2\right] \tag{9}$$

Here σ_{NS}, the Mott differential cross section, is given by the equation

$$\sigma_{NS} = \left(\frac{e^2}{2E}\right)^2 \left(\frac{\cos^2\theta/2}{\sin^4\theta/2}\right)\left(\frac{1}{1+\frac{2E}{Mc^2}\sin^2\theta/2}\right) \;, \tag{10}$$

E is the energy of the incident electron, and θ is the angle through which the electron is scattered.

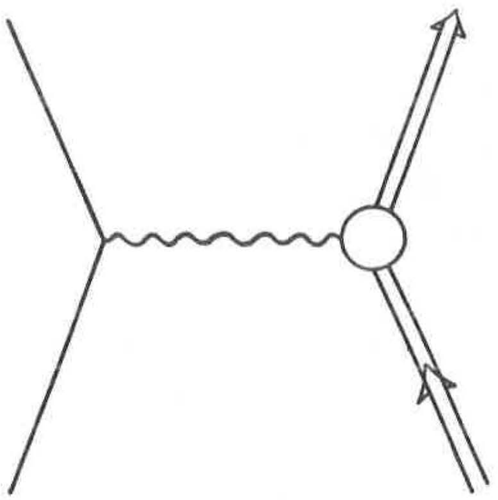

Figure 2 Feynman diagram for electron-nucleon scattering.

In terms of these variables

$$q^2 = - \frac{4\,E^2 \sin^2 \theta/2}{(\hbar c)^2 \left[1 + \frac{4E}{Mc^2} \sin^2 \theta/2\right]} \qquad (11)$$

The Feynman diagram for the Rosenbluth formula is shown in Figure 2. This calculation uses the first Born approximation and assumes that only one photon is exchanged. All of the present determinations of the nucleon form factors assume that the Rosenbluth formula describes electron-nucleon scattering. Before discussing the form factors themselves, let us look into the evidence concerning the validity of the Rosenbluth formula.

The Rosenbluth formula implies that, if one makes measurements for a fixed q^2 and a range of angles and energies, the data can be plotted so as to give a linear function of $\tan^2 \theta/2$. The equation for this line is

$$\frac{1}{\sigma_{NS}} \frac{d\sigma}{d\Omega} = \frac{G_E^2 + \tau G_M^2}{1 + \tau} + 2\tau G_M^2 \tan^2 \theta/2 \qquad (12)$$

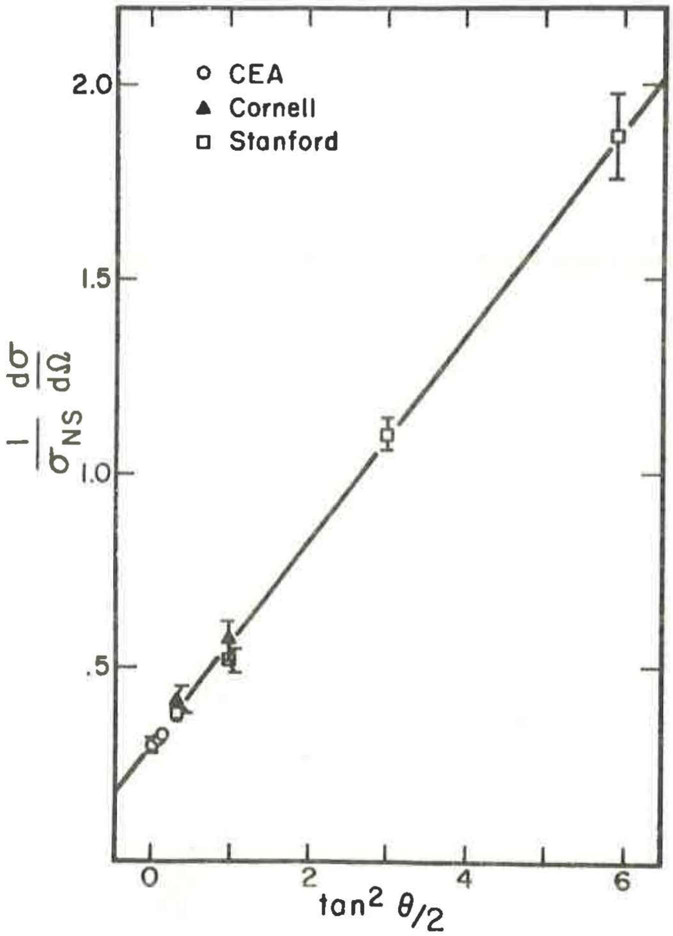

Figure 3 A Rosenbluth plot of $\frac{1}{\sigma_{NS}} \frac{d\sigma}{d\Omega}$ versus $\tan^2 \theta/2$ for $q^2 = 10\ F^{-2}$. (after R.R. Wilson and J.S. Levinger, Ref. 1).

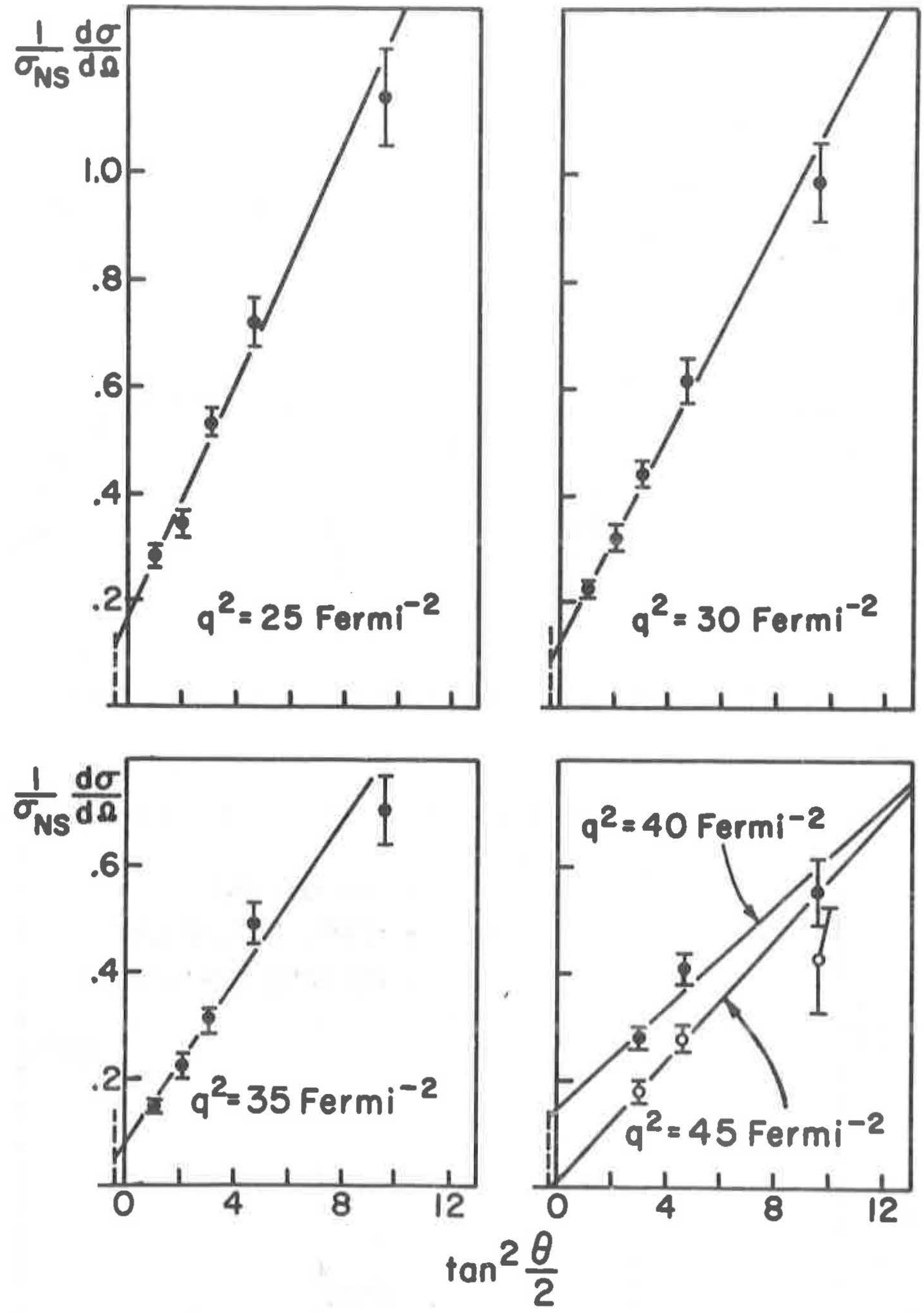

Figure 4 A plot of $\frac{1}{\sigma_{NS}} \frac{d\sigma}{d\Omega}$ versus $\tan^2 \theta/2$ for q^2 = 25, 30, 35, 40, and 45 F^{-2}.

The slope of this line gives $G_M{}^2$ and the extrapolated value at

$$\tan^2 \theta/2 = -\frac{1}{2(1+\tau)} \tag{13}$$

gives $G_E{}^2$. Such straight line plots are at present the major mode of analysis used to determine the magnetic and electric form factors from the data. This particular property[5] of the cross section can be related to the fact that in the crossed channel (annihilation) the electron-positron or nucleon-antinucleon system goes into a photon with the quantum numbers 1^-. Deviations from the Rosenbluth formula would show up as a failure of the data to lie on a straight line. One technique which has been used to check the Rosenbluth formula is to make measurements for fixed q^2 at as wide a range of energies and angles as possible. Figures 3 and 4 show plots of the data for q^2 of 10, 25, 30, 35, 40, and $45F^{-2}$.[1,6] Measurements such as this have shown no deviations from the Rosenbluth formula up to a q^2 of $50F^{-2}$. These tests can be used to set limits on the possible Regge character of the photon and on the exchange of 1^+ systems or spin 2 systems in addition to single photons.[6,7,8]

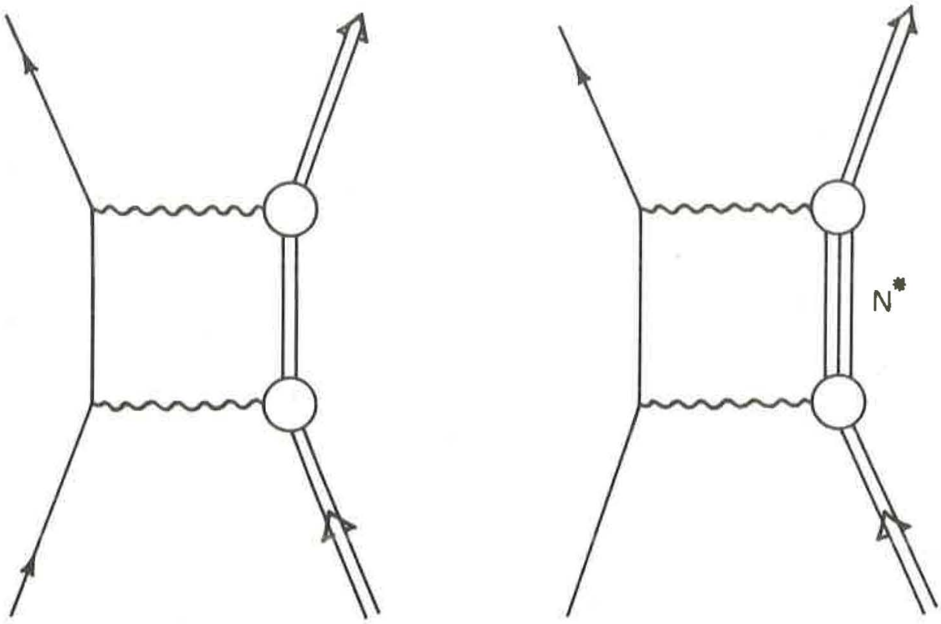

Figure 5 Feynman diagrams for two photon exchange contributions to electron scattering.

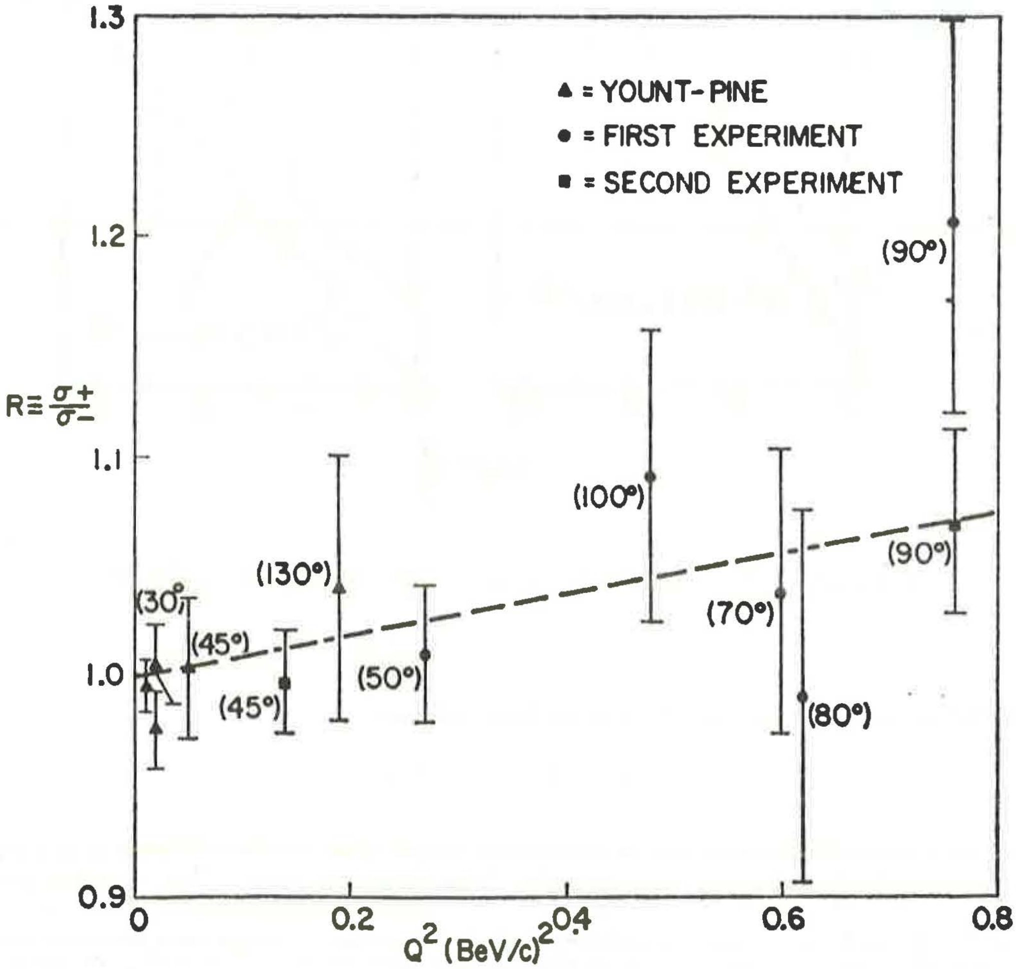

Figure 6 A summary of the experimental ratios of the positron-proton to electron-proton scattering cross section versus momentum transfer. (taken from Brownman, Liu and Schaerf, Ref. 9).

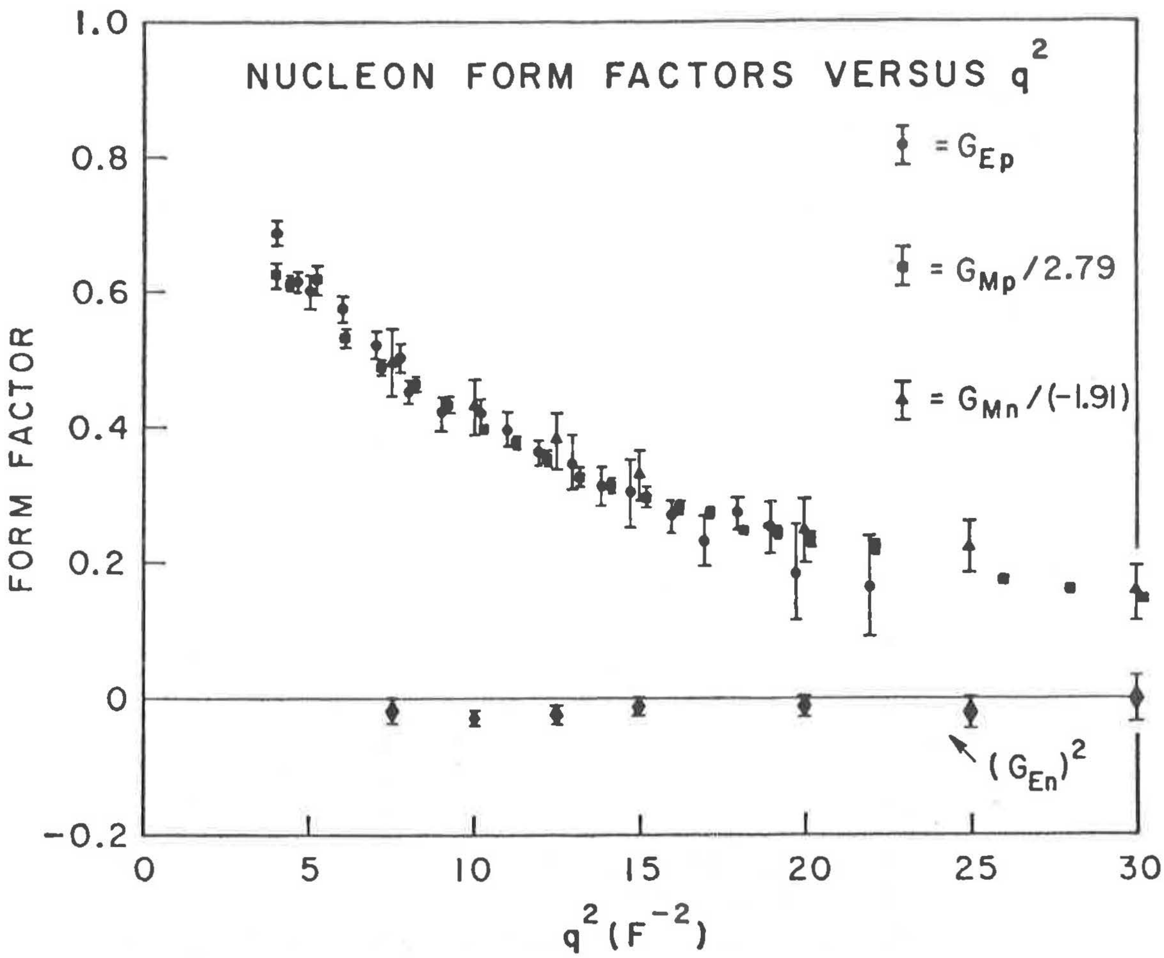

Figure 7 A comparison between the proton form factors measured by Janssens et al (Ref. 28) and the neutron form factors measured by Hughes et al (Ref. 15). (Figure taken from Ref. 15).

Another way in which deviations from Rosenbluth formula can occur is due to a breakdown of the first Born approximation and the presence of two photon exchange. Feynman diagrams for two photon exchange are shown in Figure 5. Two methods have been used to look for two photon exchange-measurements of the ratio of electron-proton to positron-proton scattering at the same energy and angle and measurements of the polarization of the recoil proton in electron proton scattering.[9,10] The first of these experiments is sensitive to the real part of the two photon amplitude, the second is sensitive to the imaginary part of the two photon amplitude. In the first Born approximation the cross sections for electron-proton and positron-proton scattering are equal and there is no polarization of the recoil proton. Figure 6 summarizes the published data on the ratio of electron-proton to positron scattering. This figure suggests that there is a small difference in the two cross sections and that it is increasing slowly with q^2. Spark chamber experiments have been carried out by Hand and Engels at Harvard and DeWire and Borgia at Cornell to check this result and to extend the measurements to higher q^2. The analysis of their data has not been completed. Measurements of the polarization of the recoil proton have been made by Bezot et al at Orsay.[11] For their experiment the energy of the incident electrons was 950 MeV and the q^2 was $16F^{-2}$. They found that the polarization of the recoil protons was 0.040 ± 0.027. Thus at present there is no evidence for a large two photon exchange amplitude. This is consistent with theoretical estimates of the two photon exchange.[12,13,14]

We now have extensive electron scattering measurements from four laboratories - Stanford, Cornell, Harvard, and Orsay. We will soon have measurements from a fifth - DESY. At these laboratories measurements are being made with a precision of a few percent and the systematic errors between laboratories are being located and reduced. One of the most striking things to come out of these new measurements is the similarity between the behavior of G_{Ep}, G_{Mp}, and G_{Mn}; they all appear to be the same function of momentum transfer. Figure 7, which was taken from a recent paper[15] by Hughes, Griffy, Yearian, and Hofstadter, shows plots of G_{Ep}, G_{Mp}/μ_p, and G_{Mn}/μ_n as a function of q^2. Figure 8 shows the data for the magnetic and electric form factors plotted in a manner which emphasizes the common dependence of the form factors on q^2. Figure 9 shows a plot which includes the higher q^2 data of the Harvard group. The Harvard group[16] has found that the data from all laboratories can be fit remarkably well by the simple expression

$$\begin{aligned} G_{Ep}(q^2) &= \frac{G_{Mp}(q^2)}{\mu_p} = \frac{G_{Mn}(q^2)}{\mu_n} = \frac{4M^2}{q^2} G_{En}(q^2) \\ &= \left(\frac{1}{1 - \frac{q^2}{18.1}}\right)^2 \qquad q^2 \text{ in } F^{-2} \\ &= \left(\frac{1}{1 - \frac{q^2}{0.72}}\right)^2 \qquad q^2 \text{ in } (\mathrm{GeV}/c)^2. \end{aligned} \tag{14}$$

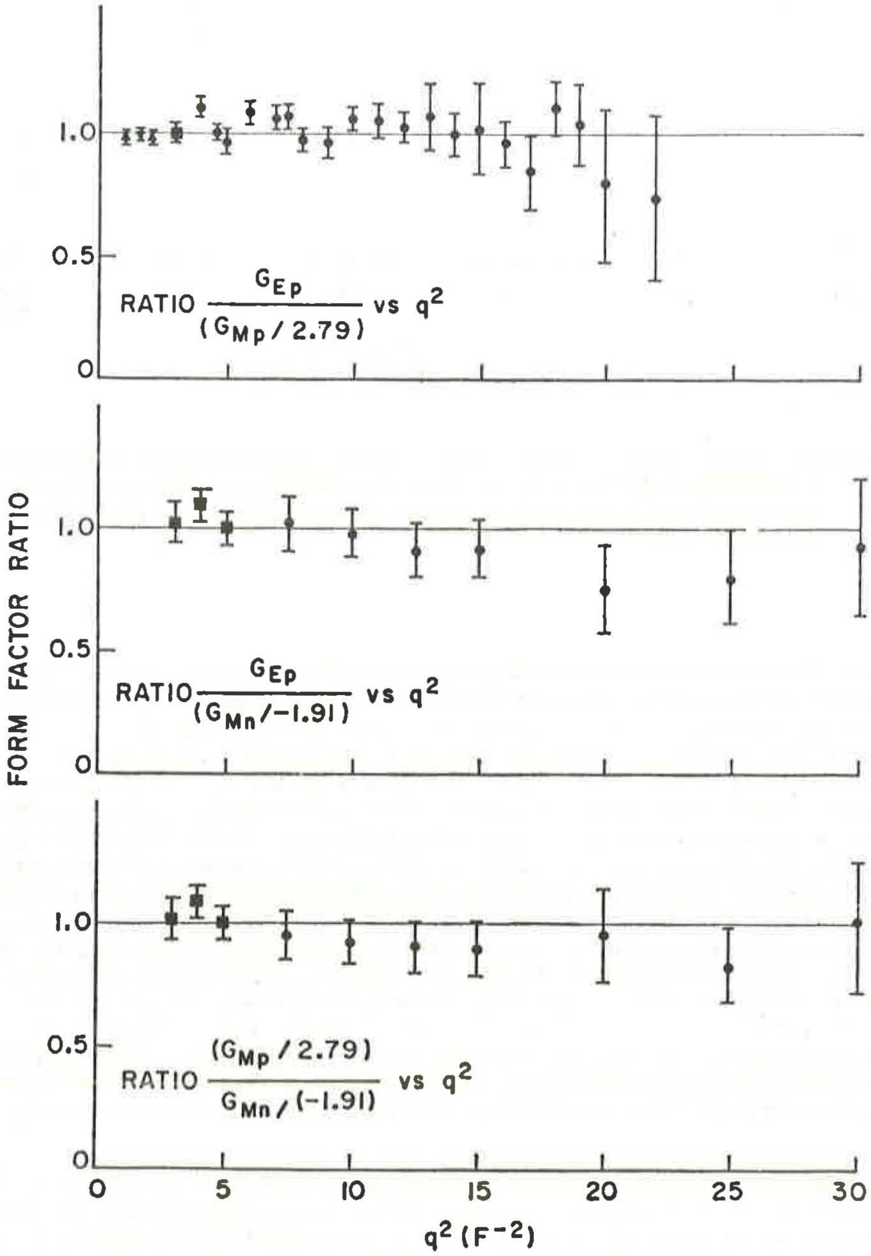

Figure 8 This figure illustrates the common dependence on q^2 of the form factors G_{Ep}, G_{Mp}, and G_{Mn}. (From Hughes et al, Ref. 15).

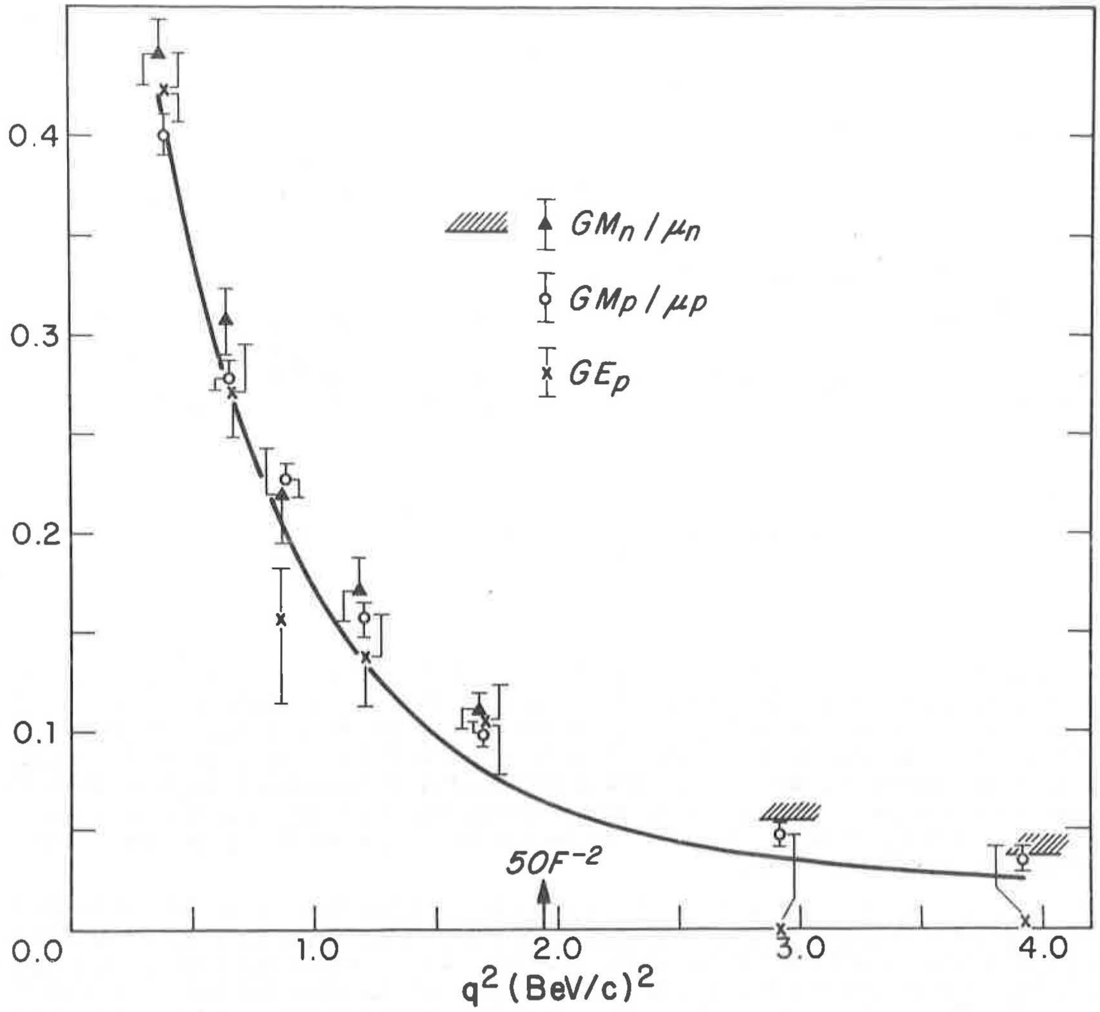

Figure 9 A figure showing the common q^2 dependence of G_{Ep}, G_{Mp}, and G_{Mn} which includes the higher q^2 data of the Harvard group. (From Dunning et al, Ref. 19).

This fit is depicted as fit #1 in Figures 13, 14, 15, and 16. There is no simple understanding of this formula. It is tempting to speculate that it is related to the relationship[17]

$$\frac{G_{Mn}(0)}{G_{Mp}(0)} = -\ ^2/_3 \tag{15}$$

predicted by unitary symmetry schemes and that it implies that one can extend the relationship 15 away from the region $q^2 = 0$. It should be noted that equations 14 are incompatible with the annihilation threshold constraint

$$G_M(4M^2) = G_E(4M^2)\ .$$

Another fact that has come out of the high q^2 measurements of the Harvard group is a much smaller upper limit on the size of any core of the nucleon.[18,19] It now appears that the nucleon has no core and that in the space-like region the form factors are going to zero like $1/q^4$.

It is natural to expect that the nucleon form factors can be explained in terms of the pion and kaon clouds around the nucleon. Attempts to relate the nucleon structure to the pions by means of dispersion relations led to the concept of a strong pion-pion interaction and the rho meson. Since then many mesonic and baryon resonance states have been discovered and it has become popular to try to explain the nucleon form factors in terms of the vector mesons with the same quantum numbers as the gamma ray. Since isotopic spin is a good quantum number for the vector mesons, it is assumed that the isovector and isoscalar form factors can be expressed in terms of the isovector and isoscalar vector mesons. Thus it is assumed for example that[20,21,22,23]

$$G_V = \sum_i \frac{e\, g_{v_i NN}}{2\,\gamma_{V_i}} \frac{M_i^2}{M_i^2 - q_i^2} = \sum_i \frac{\alpha_i}{1 - \frac{q_i^2}{M_i^2}} \tag{16}$$

The constant γ_v is a measure of the coupling of the vector meson to the gamma ray. It can be determined by measuring the decay rate of the vector meson into lepton pairs. In terms of γ_v the decay rate into lepton pairs is

$$\Gamma_{V \rightarrow l\bar{l}} = \frac{\alpha^2}{\gamma_V^2/4\pi} \frac{M_V}{12} \left[1 + \text{order of} \left(\frac{M_l^4}{M_V^4} \right) \right]$$

The constant g_{VNN} is the coupling constant for the vector-meson nucleon interaction.

This particular expansion formula is a special case of a general dispersion theory expression for the nucleon form factors. Dispersion theory arguments suggest that if q^2 is generalized to a complex momentum transfer variable, Z, the form factors are an analytic function of Z with a branch cut along the positive real axis from $4m^2$ to ∞. If G_v vanishes sufficiently rapidly at ∞, we can write for G_v the unsubtracted dispersion relation

$$G_V(q^2) = \frac{1}{\pi} \int_{4m_\pi^2}^{\infty} \frac{\mathrm{Im}\, G_V(q'^2)}{(q')^2 - q^2}\, d(q')^2 \qquad (17)$$

The weight function Im $G_v(q'^2)$ is related to the matrix elements for processes in which a photon couples to intermediate states of total mass $(q')^2$ which in turn annihilate to form a nucleon-antinucleon pair. It has not been proved that the form factors possess the analyticity properties implied by Equation 17.[24] General field theoretic arguments suggest that the exact shape of the domain of analyticity of the actual form factors is a complicated function of the masses involved. In view of these arguments it is not clear just what the exact significance of the pole analysis is. It does, however, give a convenient way to represent the data and the representation may have a simple interpretation in some future theory.

The only well established vector meson is the ρ with a mass of 760 MeV and a width of 100 MeV. The well established isotopic scalar mesons are the ω with a mass of 782 MeV and a width of 10 MeV and the φ with a mass of 1020 MeV and a width of 3 MeV. Most of the analyses of the form factors in terms of the vector mesons have not taken the width into consideration but have simply used equations of the form of Equation 16. The first fit which we shall consider is a three pole fit by Hughes et al. They assumed that the form factors could be expanded in the form

$$\begin{aligned}
G_{ES} &= 0.5 \left\{ \frac{S_{e1}}{1 - \frac{q^2}{15.7}} + \frac{S_{e2}}{1 - \frac{q^2}{26.7}} + (1 - S_{e1} - S_{e2}) \right\} \\
G_{MS} &= 0.44 \left\{ \frac{S_{m1}}{1 - \frac{q^2}{15.7}} + \frac{S_{m2}}{1 - \frac{q^2}{26.7}} + (1 - S_{m1} - S_{m2}) \right\} \\
G_{EV} &= 0.5 \left\{ \frac{\nu_{e1}}{1 - \frac{q^2}{M_\rho^2}} + (1 - \nu_{e1}) \right\} \\
G_{MV} &= 2.353 \left\{ \frac{\nu_{m1}}{1 - \frac{q^2}{M_\rho^2}} + (1 - \nu_{m1}) \right\}
\end{aligned} \qquad (18)$$

These equations assume that the isoscalar form factors can be expressed in terms of the ω, the φ, and a core contribution due to higher mass states or nonresonance intermediate states. These equations assume that the isovector form factors can be expressed in terms of a ρ whose mass is adjusted to fit the data and a core term. In making their fit Hughes et al[15] imposed the condition

$$\left(\frac{dG_{En}}{dq^2} \right)_{q^2=0} = 0.021\ F^{-2}$$

as required by the measured neutron-electron interaction[25,26,27] and fit the electron-proton scattering cross sections measured by Janssens[28] and the elastic electron-proton to quasi-elastic electron deuterium ratios measured by themslves. The fit they obtained was

$$G_{ES} = 0.5\left\{\frac{2.18 \pm 0.06}{1 - \frac{q^2}{15.7}} - \frac{1.11 \pm 0.14}{1 - \frac{q^2}{26.7}} - 0.07 \pm 0.15\right\} \tag{19}$$

$$G_{MS} = 0.44\left\{\frac{2.42 \pm 0.05}{1 - \frac{q^2}{15.7}} - \frac{1.35 \pm 0.09}{1 - \frac{q^2}{26.7}} - 0.07 \pm 0.15\right\}$$

$$G_{EV} = 0.5\left\{\frac{1.05 \pm 0.07}{1 - \frac{q^2}{(7.51 \pm 0.32)}} - 0.05 \pm 0.07\right\}$$

$$G_{MV} = 2.353\left\{\frac{1.05 \pm 0.01}{1 - \frac{q^2}{(7.51 \pm 0.32)}} - 0.05 \pm 0.01\right\}$$

Figure 10 shows how well this fit represents the data for the isovector and isoscalar form factors. Figures 11 and 12 show how well this fit represents the form factors of the neutron and proton when data other than that used in making the fit is included. It is interesting that with the exception of G_{MV}

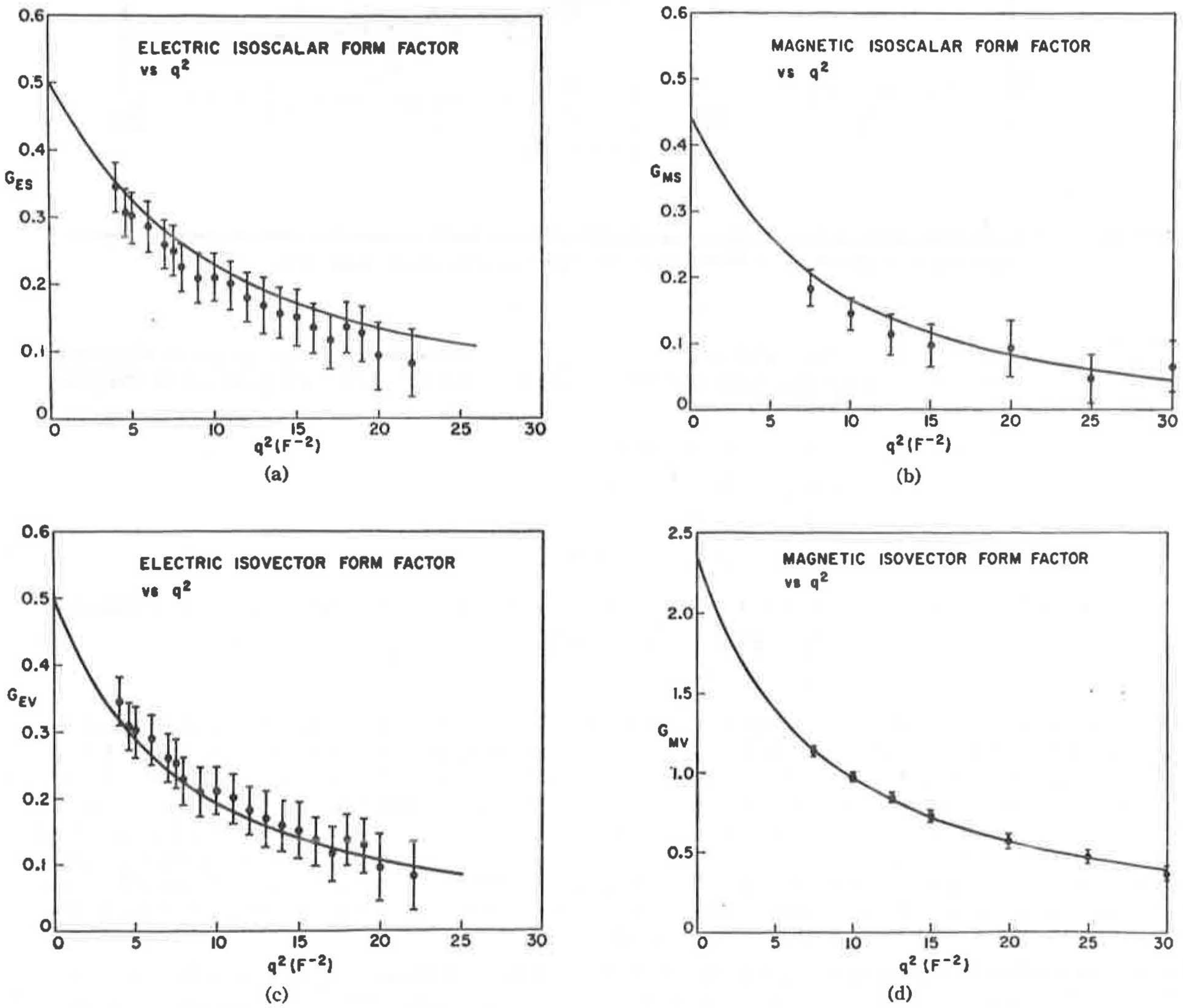

Figure 10 Plots showing a comparison between the three pole fit of Hughes et al (Ref. 15) and the measured isovector and isoscalar form factors. (From Hughes et al, Ref. 15).

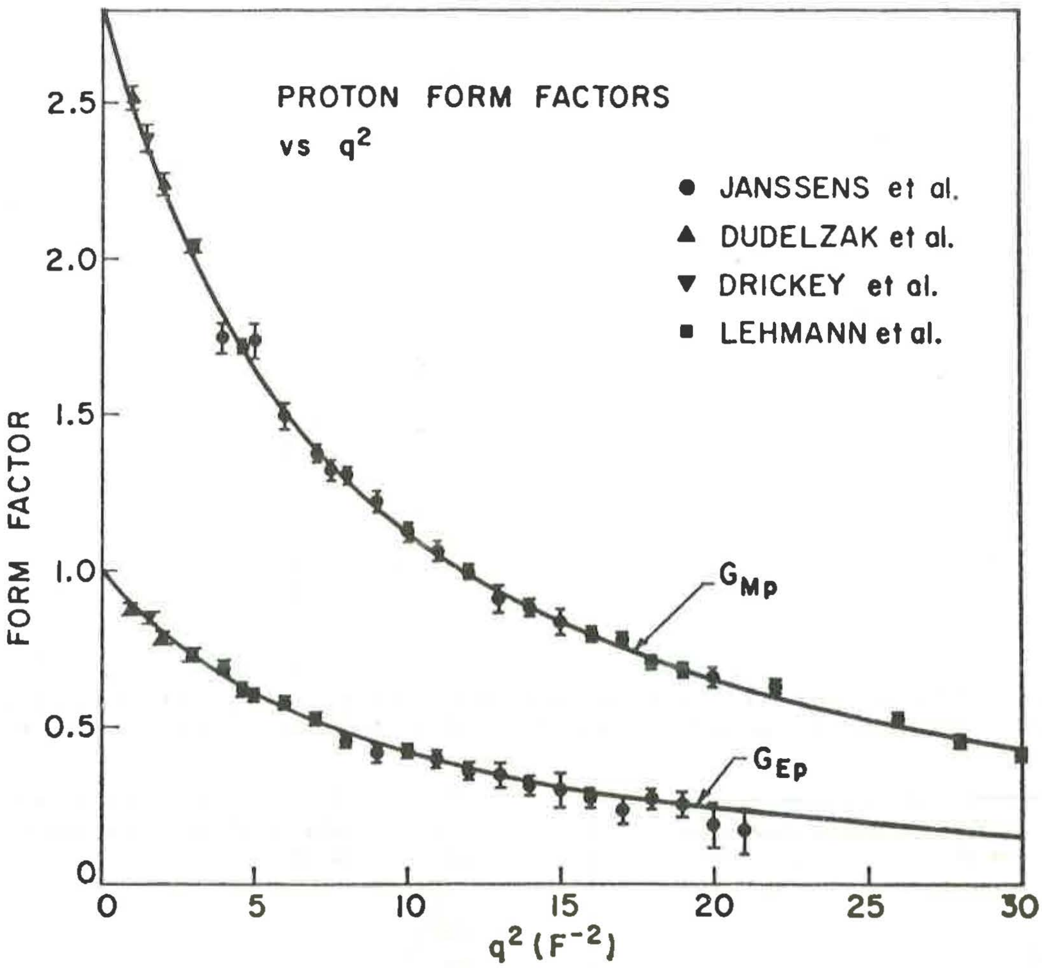

Figure 11 A comparison between the experimental form factors for the proton and the three pole fit of Hughes et al (Ref. 15). (From Hughes et al, Ref. 15).

the constant or core terms are zero within the error of the fit and that the optimum fit is obtained for an effective mass of the ρ meson equal to 548 $\pm$ 24 MeV. If the fits are extrapolated to the point $q^2 = 4M^2$, the form factors obtained are

$$G_{ES} = 0.03 \pm 0.15,$$
$$G_{MS} = 0.19 \pm 0.08,$$
$$G_{EV} = -0.10 \pm 0.05,$$
$$G_{MV} = -0.38 \pm 0.15.$$

This implies that within the errors the fits are consistent with the annihilation threshold constraint

$$G_{ES}\,(4M^2) = G_{MS}\,(4M^2),$$
$$G_{EV}\,(4M^2) = G_{MV}\,(4M^2).$$

Chan et al[16] at Harvard have made a more general study of how the pole model can be used to fit the electron scattering data. They included in their fits data from Stanford, Cornell, Orsay and the Cambridge Electron Accelerator. They included the measurements of the electron-neutron interaction and rejected some measurements of the elastic electron-deutron scattering on the basis that the theory may be inadequate. Chan et al made a three pole fit similar to that employed by Hughes et al. They used isoscalar poles at the ω and φ masses, a single isovector pole whose mass was adjusted for the best fit, and hard core terms. This fit is shown as fit 3 in Figures 13, 14, 15, and 16. Chan et al found this fit gave for the ρ mass a value of 540 MeV. They also found that this fit systematically failed to fit the high momentum transfer points.

Chan et al found that their best fit was a four pole resonance fit without core terms. This is shown as fit 4 in Figures 13, 14, 15, and 16. In this fit they used isoscalar poles at the ω and φ masses, one isovector pole at the measured ρ mass and a second isovector pole whose mass was adjusted in the fitting process. They required the form factors to satisfy the constraint at the annihilation threshold. It was found that the fit did not improve greatly by including cores or releasing the annihilation threshold constraint. The relationship $G_{Ep} = G_{Mp}/\mu_p$ is not particularly well satisfied by this fit at momentum transfers above 0.5 (GeV/c). The mass found for the additional isovector meson was 875 MeV. In terms of this fit the isoscalar and isovector form factors are given by the equations

$$
\begin{aligned}
G_{ES} &= \left\{ \frac{1.214}{1 - \frac{q^2}{15.7}} - \frac{0.714}{1 - \frac{q^2}{26.7}} \right\} ; \\
G_{MS} &= \left\{ \frac{1.093}{1 - \frac{q^2}{15.7}} - \frac{0.653}{1 - \frac{q^2}{26.7}} \right\} ; \\
G_{EV} &= \left\{ \frac{2.347}{1 - \frac{q^2}{14.9}} - \frac{1.847}{1 - \frac{q^2}{19.7}} \right\} ; \\
G_{MV} &= \left\{ \frac{8.164}{1 - \frac{q^2}{14.9}} - \frac{5.811}{1 - \frac{q^2}{19.7}} \right\} .
\end{aligned}
\tag{20}
$$

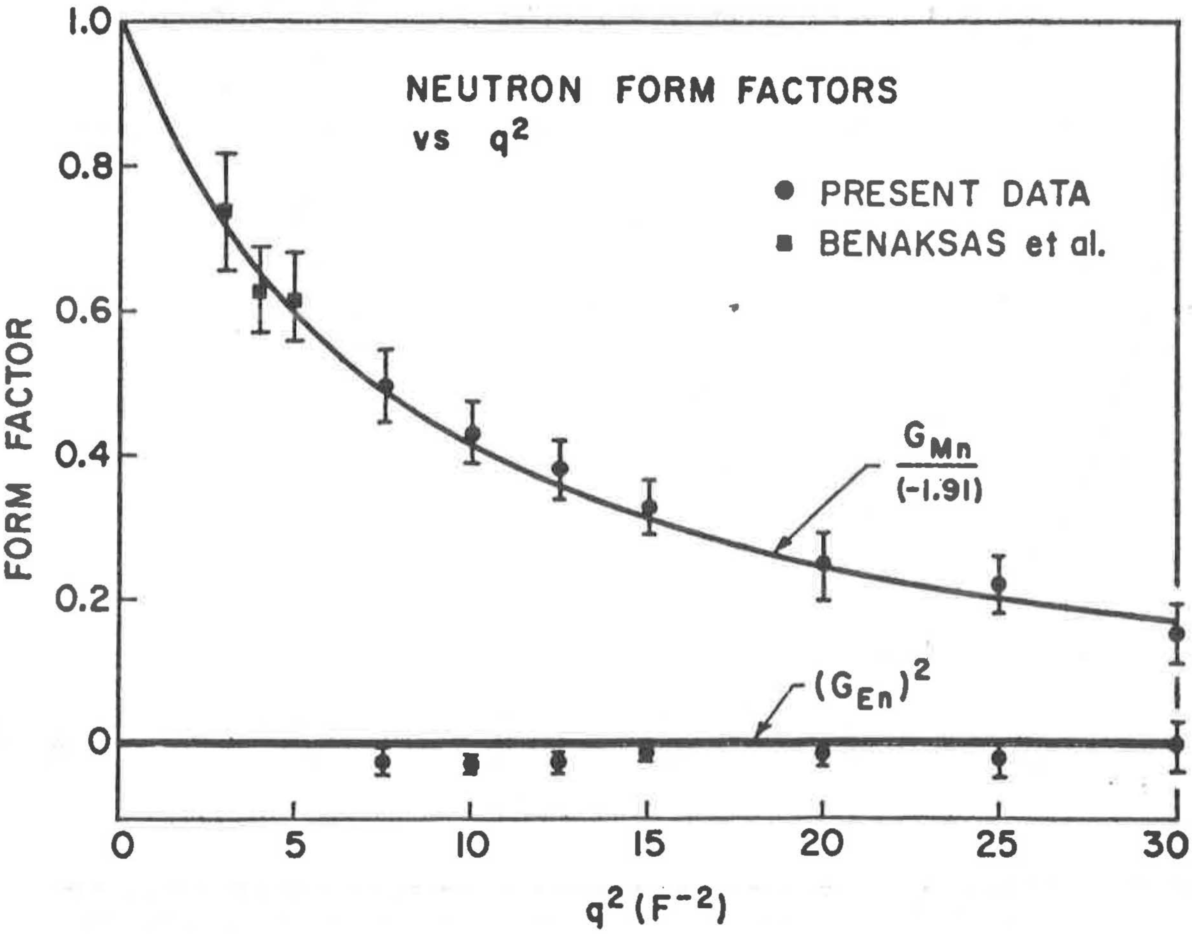

Figure 12 A comparison between the experimental form factors for the neutron and the three pole fit of Hughes et al (Ref. 15). (From Hughes et al, Ref. 15).

From these various fits it is concluded that one cannot understand the form factors with a simple resonance model using the observed masses of only the ω, φ, and ρ vector mesons. In order to obtain a satisfactory fit it is necessary to either make the effective mass of the ρ much smaller or to include a second isovector meson with a mass greater than that of the ρ. There appears to be no necessity to include core terms, and the annihilation threshold constraint has very little effect upon the fit.

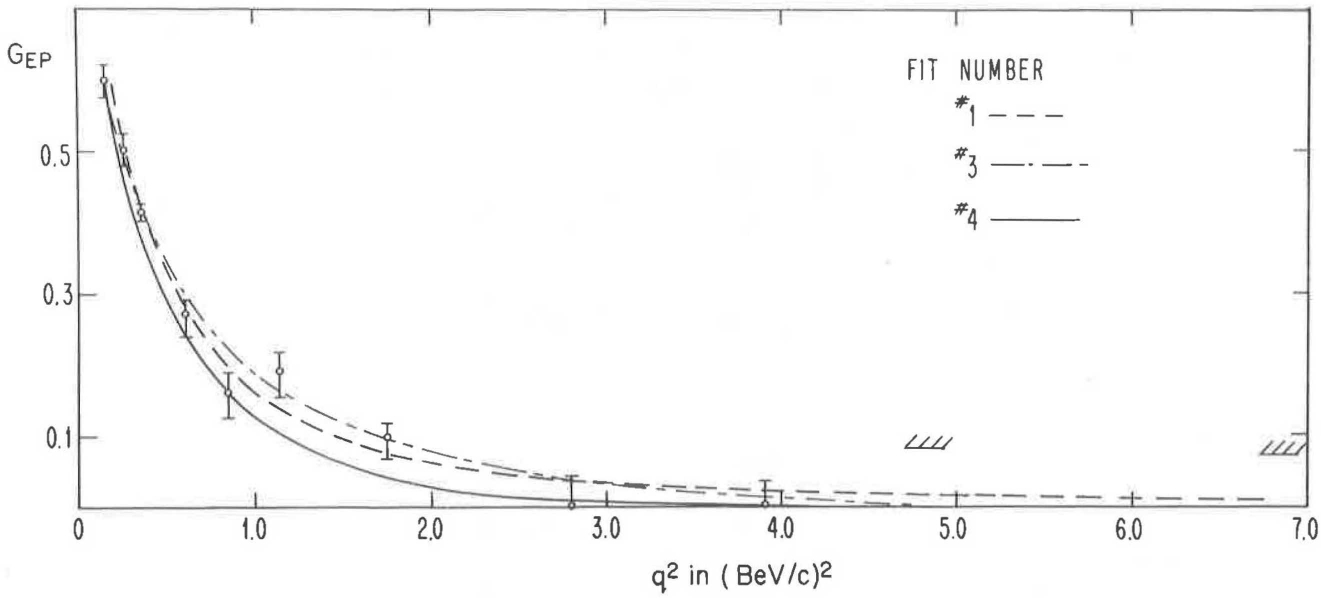

Figure 13 A comparison of the experimental data for G_{Ep} and three of the fits by Chan et al. (Ref. 16). Fit one is the one parameter fit of Equations 14; fit three is a three pole fit similar to that employed by Hughes et al (Ref. 15); fit four is a four pole fit using two isoscalar and two isovector mesons. (From Chan et al, Ref. 16).

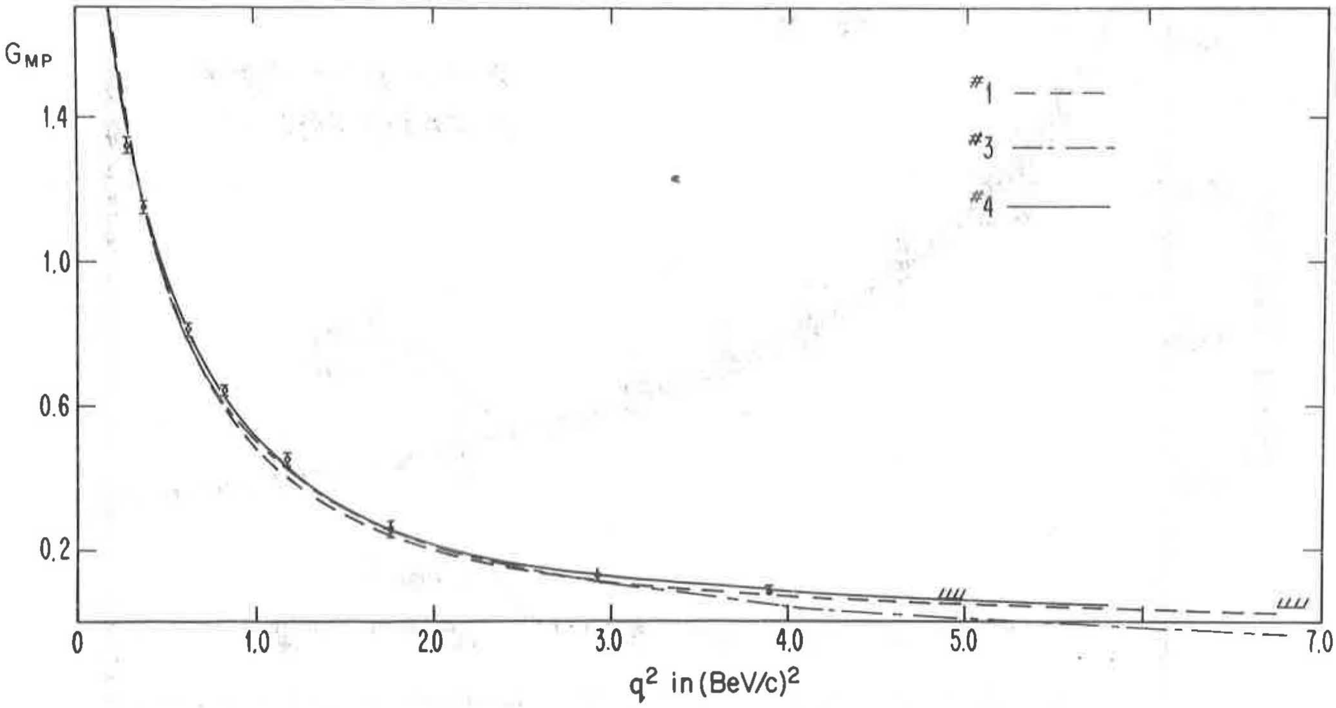

Figure 14 A comparison of the experimental data for G_{Mp} and three of the fits by Chan et al (Ref. 16). The notation is the same as for Fig. 13. (From Chan et al, Ref. 16).

Several kinds of experiments can be used to understand further the role of the vector mesons in the nucleon form factors. One of the most helpful measurements would be the decay rate of the ρ, ω, and φ into electron and muon pairs. This information would make in possible to determine the vector meson-nucleon coupling constants from the electron scattering fits. These coupling constants could then be compared with the estimates from strong interaction experiments. A measurement of the decay rate of the vector meson into both meson and electron pairs would also give a new test of quantum electrodynamics in the time-like region.

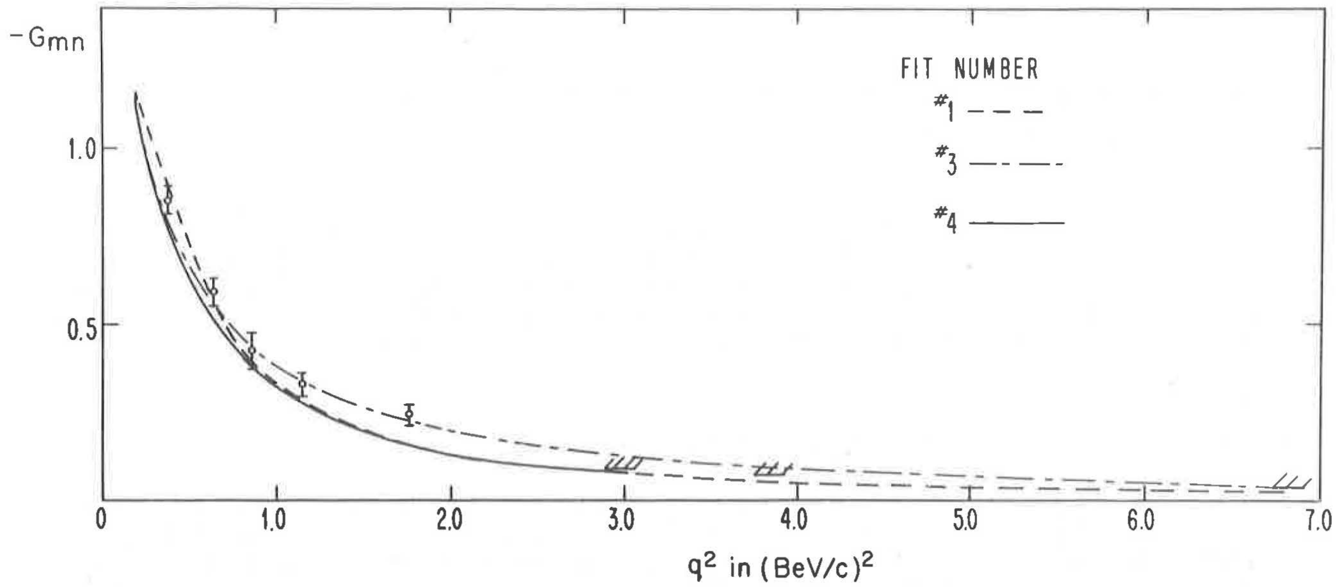

Figure 15 A comparison of the experimental data for G_{Mn} and three of the fits of Chan et al. (Ref. 16). The notation is the same as for Figure 13. (From Chan et al, Ref. 16).

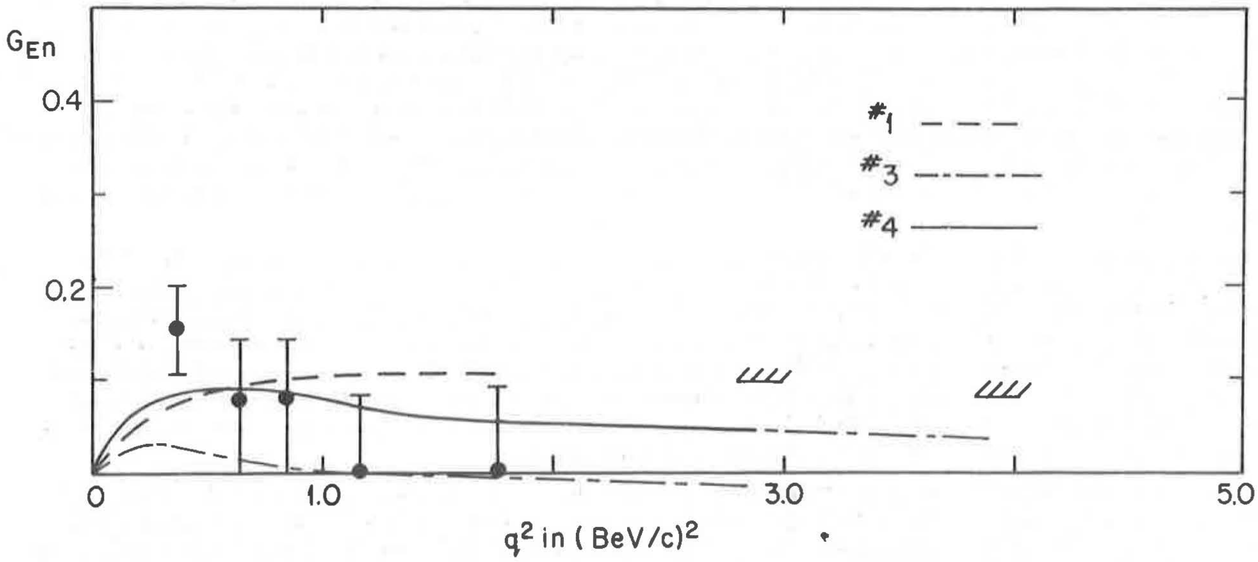

Figure 16 A comparison of the experimental data for G_{En} and three of the fits by Chan et al (Ref. 16). The notation is the same as for Figure 13. (From Chan et al, Ref. 16).

Another valuable source of information on the nucleon form factors is measurements of proton-antiproton annihilation into electron-positron or muon-antimuon pairs. The total cross section for proton-antiproton annihilation into electron positron pairs is[29]

$$\sigma_T(p\bar{p} \to e\bar{e}) = \frac{\pi \alpha^2}{6 M^2 \tau^2} \left(\frac{\tau}{1+\tau}\right)^2 \quad \{ |G_E(q^2)|^2 - 2\tau \, |G_M(q^2)|^2 \} \tag{21}$$

where

$$q^2 = 2M(E_{\bar{p}} + M) \ , \tag{22}$$

and

$$\tau = - \frac{q^2}{4M^2} = - \frac{E_{\bar{p}} + M}{2M} \tag{23}$$

Here $E_{\bar{p}}$ is the total energy in the laboratory system of the antiproton incident upon a proton at rest. Experiments are now in progress at Brookhaven and CERN using incident antiprotons with a momentum of roughly 2.5 Gev/c. $q^2 = 5.4$ (Gev/c)^2

Conversi, Massam, Muller, and Zichichi (CERN) reported at this conference their results for $q^2 = 6.8\ (\mathrm{Gev}/c)^2$. They observed muon pairs for 1.4×10^{10} incident antiprotons and electrons for 0.4×10^{10} incident antiprotons. Their results were consistent with there being no real events. They used the muon data to set an upper limit to the form factors. They found that

$$\frac{\sigma_{\mu\mu}\ \text{experimental}}{\sigma\ \text{point}} \leqslant 3.0 \times 10^{-3}$$

If it is assumed that $|G_{Ep}| = 0$, this gives an upper limit for $|G_{Mp}|$ of 0.21; if it is assumed that $|G_{Mp}| = 0$ this gives an upper limit for $|G_{Ep}|$ of 0.31; if it is assumed that $|G_{Ep}| = |G_{Mp}|$ this gives an upper limit of 0.18 for $|G_{Ep}|$. If the form factors in the time-like region are everywhere as small as these results suggest, experiments on electron-positron annihilation into nucleon-antinucleon pairs will be difficult to perform with the presently contemplated electron-positron storage rings.

Investigation of Quantum Electrodynamics

The most successful theory that we have at present is quantum electrodynamics[30]. This theory deals with the interaction of charged particles and the electromagnetic field. As near as we can tell, it describes completely the structure of the electron and the muon; using this theory we can predict very precisely the details of atomic spectroscopy. The theory has, however, a logical shortcoming. When certain quantities such as the correction to the mass of the electron due to its interaction with the electromagnetic field are calculated, an infinite answer is obtained. One of the great triumphs of post World War II theoretical physics was the reformulation of quantum electrodynamics in such a fashion as to extract the finite, measureable part of these infinities. This reformulation is called renormalization theory and it proceeds, for example, by showing that the infinite self mass correction can be added to the bare mass which enters the uncoupled theory and the sum of the two replaced by the finite experimental mass. Just what all this means has been a source of speculation. It is clear that electrodynamics is incomplete and that ultimately it must become linked with the other particles. Perhaps the infinities are due only to the incompleteness of the theory. There has also been speculation that there is some fundamental length which gives a natural cut off at small distances. It is an open question whether this length depends upon the strong, the weak, or the gravitational interaction. In this section I wish to review the present evidence for the validity of quantum electrodynamics.

The best evidence for the validity of quantum electrodynamics comes from measurements of the Lamb shift in hydrogen-like atoms and the gyromagnetic ratios of the electron and the muon. Less precise evidence comes from measurements of the hyperfine structure of muonium and hydrogen and the separation between the singlet and triplet 1s states in positronium. The best value for the fine structure constant comes from the measurements by Lamb of the fine structure of atomic deuterium. Of these measurements the muon g-factor tests the theory at the highest momentum transfers. Until quite recently all of these measurements were in complete agreement with theory. There appears now, however, to be some evidence of disagreement.

The Lamb shift in hydrogen is the separation between the n = 2, $^2S_{\frac{1}{2}}$ state and the n = 2, $^2P_{\frac{1}{2}}$ state. These states are degenerate in the Dirac theory and their separation is explained by higher order interactions with the electromagnetic field. The dominant contribution to the Lamb shift comes from electromagnetic corrections to the electron mass. The most recent, published, theoretical value for the Lamb shift is Layzer's calculation[31]

$$S_{th} = 1057.70 \pm 0.15\ \mathrm{Mc/sec}$$

This value takes into account terms of order $\alpha(Z\alpha)^6 \ln^2 Z\alpha$ and $\alpha(Z\alpha)^6 \ln Z\alpha$. A more recent but unpublished calculation by Erickson gives the value[32]

$$S_{th}{}^1 = 1057.64 \pm 0.15\ \mathrm{Mc/sec}$$

The best experimental value of Lamb and his co-workers is[33]

$$S_{Lamb} = 1057.77 \pm 0.10\ \mathrm{Mc/sec}$$

This value is in very good agreement with the theory. A new measurement of the Lamb shift has recently been reported by Robiscoe. Robiscoe found[34]

$$S_{Robiscoe} = 1058.07 \pm 0.10\ \mathrm{Mc/sec}$$

This value differs from the Lamb value and from theory by three times the rms error. A recent comparison by Erickson[35,36] of the theoretical and experimental values of the Lamb shift in Li^{++} suggests that there is no error in the Z dependent theoretical terms. The resolution of this discrepancy in hydrogen requires further experimental and theoretical work.

The theoretical value for the g-factor of the electron is[37,38]

$$\frac{g-2}{2} = \frac{\alpha}{2\pi} - 0.328\,\frac{\alpha^2}{\pi^2} \tag{24}$$

Recently Drell and Pagels have reported a dispersion theory calculation in which they estimate the next term as[39]

$$+\,0.15\,\frac{\alpha^3}{\pi^3} \tag{25}$$

The best experimental value is[40]

$$\frac{g-2}{2} = 0.001159622 \pm 0.000000027$$

In terms of the fine structure constant determined by Lamb and co-workers from measurements of the deuterium fine structure[41,42]

$$\alpha^{-1} = 137.0388 \pm 0.0012$$

and

$$\frac{g-2}{2} = \frac{\alpha}{2\pi} - (0.327 \pm 0.005)\,\frac{\alpha^2}{\pi^2}$$

The experiment thus completely confirms the theory. It will require a better value of the fine structure constant to make it possible to check the third order term calculated by Drell and Pagels.

The theoretical value for the correction to the g-factor of the muon is[43,44]

$$\frac{g-2}{2} = \frac{\alpha}{2\pi} + 0.76\,\frac{\alpha^2}{\pi^2} \tag{26}$$

The best experimental value is[45]

$$\frac{g-2}{2} = 0.001162 \pm 0.000005.$$

Here again the theory and experiment are in agreement.

The theoretical value for the separation between the singlet and triplet 1s states of positronium is[46]

$$2.0337 \times 10^5 \text{ Mc/sec}$$

The experimental value of Weinstein, Deutsch, and Brown is[47]

$$(2.0338 \pm 0.0004) \times 10^5 \text{ Mc/sec}$$

This measurement is interesting in that it confirms the presence of the term in which the electron and positron virtually annihilate into a photon and then reappear.

The theoretical value for the hyperfine splitting of muonium is[48]

$$\Delta\nu_M = 2.632936 \times 10^7\,\alpha^2 \left(\frac{\mu_\mu}{\mu_p}\right) \text{ Mc/sec} \qquad (\pm 1.5 \text{ ppm})$$

$$= 4463.15 \pm 0.10 \text{ Mc/sec} \qquad (\pm 22 \text{ ppm})$$

The dominate uncertainty is due to the uncertainty in α. Cleland et al at Yale measured the hyperfine splitting of muonium and found the value

$$(\Delta\nu)_M \text{ (exp)} = 4463.15 \pm 0.06 \text{ Mc/sec } (\pm 13 \text{ ppm})$$

The Yale group used this measured splitting together with the theoretical formula to determine α. They found an α in agreement with that determined by Lamb, namely

$$\alpha^{-1} = 137.0388 \pm 0.0012.$$

The hydrogen hyperfine splitting arises from the interaction of the proton magnetic moment with the magnetic field due to the electron. This splitting has been measured to two parts in 10^{11} and is one of the most precisely known experimental constants. The theoretical formula for the hydrogen hyperfine splitting is

$$(\Delta\nu)_H = \frac{16\alpha^2 cR_\infty}{3}\left(\frac{\mu_p}{\mu_e}\right)\left(1+\frac{M_e}{M_p}\right)^{-3}(1+a_e)^2(1+\epsilon_1+\epsilon_2)(1-\delta_p) \tag{27}$$

Here

$$a_e = \frac{\alpha}{2\pi} - 0.328\,\frac{\alpha^2}{\pi^2}\ ,$$

$$\epsilon_1 = -(1-\ln 2)\alpha^2\ ,$$

$$\epsilon_2 = -\frac{8\alpha^3}{3\pi}\ln\alpha\left(\ln\alpha - \ln 4 + \frac{281}{480}\right)\ .$$

δ_p is a term which accounts for proton recoil and proton structure. The two principal uncertainties in this expression are δ_p and α^2. Using their measured muonium hyperfine splitting, Cleland et al[48] found

$$\delta_p = (-9 \pm 18) \times 10^{-6}.$$

Iddings has carefully re-examined the calculation of the proton size correction.[49] He finds

$$\delta_p = (35 \pm 3) \times 10^{-6}.$$

This seems to suggest that either the Lamb value of α and the Cleland measurement of the muonium hyperfine structure are in error or that the structure correction for the proton is not theoretically understood. One can question all three aspects. More recent adjustments of the atomic constants incorporating double crystal spectrometer measurements of the wavelength of annihilation radiation to determine α suggest that the Lamb value of α may be too small. In their determination of the muonium hyperfine structure interval, Cleland et al made measurements at various pressures of argon and extrapolated to zero pressure. The pressure shift they obtained disagrees with more recent measurements of the pressure shift of the hydrogen hyperfine splitting. If the somewhat larger pressure shift obtained from measurements on hydrogen and tritium is used to analyze the Cleland data on muonium, one obtains a larger muonium hyperfine splitting and a value for the proton structure factor more in agreement with theory. The calculation of the proton structure factor is difficult because it involves the spin-flip amplitude for two-photon exchange.

One can summarize the present state of these atomic physics type verifications of quantum electrodynamics by saying that the agreement is by no means air tight. Much remains to be done and all the measurements should be checked. It would be especially valuable to have an independent and more precise value for the fine structure constant.

If we accept the premise that these experiments verify quantum electrodynamics for low momentum transfer, then we can ask in addition what they tell us about the high momentum behavior. Each of these calculations such as that for the correction to the g-factor involve integrations over virtual momenta. If the theory is to alter its structure at high energy, then these cut-off parameters should appear in the virtual integrations. In order to see just what these measurements tell us about the high momentum behavior, it is necessary to introduce some kind of a model for the breakdown of quantum electrodynamics at high momentum transfers.

High momentum transfer corrections to quantum electrodynamics could show up as modifications of the photon propagator, the electron or muon propagator, and the electron or muon vertex. In a certain sense a modification of the photon propagator could be intrepreted as a deviation from the Coulomb force law at small distances, a modification of the lepton propagator could be interpreted as a change in the lepton mass, and a modification of the electron or muon vertex could be interpreted as a finite extension of the lepton. The most common technique used to modify the photon propagator is to make the replacement[50,51,52]

$$\frac{1}{q^2} \to \frac{1}{q^2} - \frac{1}{q^2-\Lambda^2} = \frac{1}{q^2}\left(\frac{1}{1-\frac{q^2}{\Lambda^2}}\right) \tag{29}$$

If this form of the propagator is used in the integration over virtual momenta, the final result will be a function of Λ and the agreement between experiment and theory can be used to set a limit on the cut-off parameter Λ. A completely analogous technique can be used to modify the electron or muon propagator and the electron or muon vertex. The only trouble with this method is that these modifications are not always in accord with general theorems concerning field theory and as a result have a questionable meaning. This has been particularly emphasized in a recent paper by McClure and Drell.[53] For the photon propagator there exists the general spectral representation[54]

$$D'(k^2) = \frac{1}{k^2} + \int_0^\infty \frac{\pi(\sigma^2)}{k^2 - \sigma^2} \, d\sigma^2 \tag{30}$$

where $\pi(\sigma^2)$ is a positive function which is related to the cross section for creating particle-antiparticle pairs of mass σ^2. Equation 29 does not satisfy this representation. We should use instead

$$\frac{1}{q^2} \rightarrow \frac{1}{q^2} + \frac{1}{q^2 - \Lambda^2} \tag{31}$$

The situation is even more complicated for the case of the electron propagator. The Ward-Takahashi identity gives the following general relationship between the electron propagator and the electron-gamma ray vertex function,[55,56]

$$S_F(p')\, q^\mu\, \Gamma_\mu(p', p, q)\, S_F(p) = S_F(p) - S_F(p') \ . \tag{32}$$

This relationship follows from current conservation and gauge invariance. To be consistent a modification of the lepton propagator must be accompanied by a corresponding modification of the vertex. In most Feynman diagrams, the electron propagator has one end at a vertex so there can be cancellations between the propagator correction and the vertex correction. One can illustrate this with examples taken from McClure and Drell. The Feynman diagram for the first order correction of the electron g-factor is shown in Figure 17. If the propagator of the virtual photon is replaced by the regulated propagator of equation 29 the correction to the lepton g-factor becomes[53]

$$\frac{g-2}{2} = \frac{\alpha}{2\pi}\left[1 - \frac{2}{3}\left(\frac{m}{\Lambda}\right)^2\right] \ . \tag{33}$$

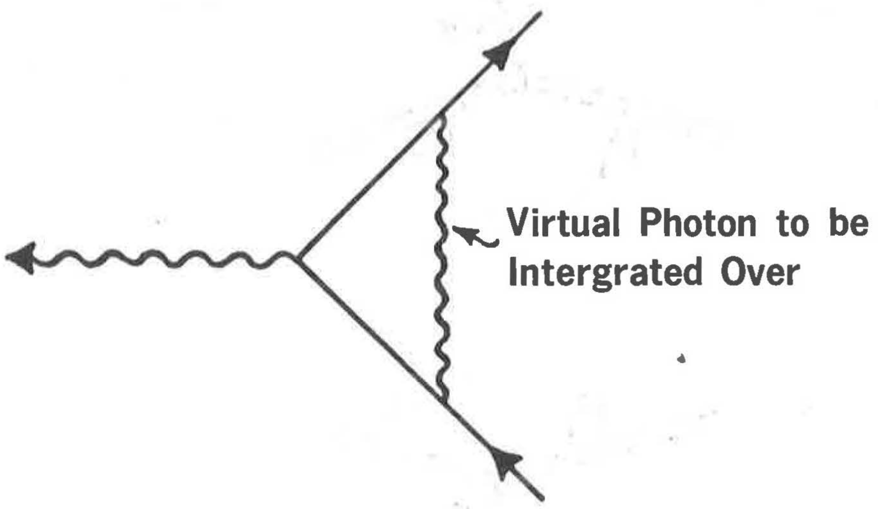

Figure 17 A Feynman diagram for the α correction to the g-factor of a lepton.

The use of the expression in equation 31 for the propagator of the virtual photon changes the correction to[53]

$$\frac{g-2}{2} = \frac{\alpha}{2\pi}\left[1 + \frac{2}{3}\left(\frac{m}{\Lambda}\right)^2\right] \tag{34}$$

One can also modify the propagator for the virtual lepton or introduce a vertex correction. Consider the case where the propagator of the virtual lepton is replaced by the expression[51]

$$\frac{1}{p^2 - m^2} \rightarrow \frac{1}{p^2 - m^2} - \frac{1}{p^2 - m^2 - \Lambda_2^2} = \frac{1}{p^2 - m^2}\left(\frac{1}{1 - \frac{p^2 - m^2}{\Lambda_2^2}}\right) \tag{35}$$

If one calculates the correction to the g-factor using only this modified propagation, one fines that[51]

$$\frac{g-2}{2} = \frac{\alpha}{2\pi}\left(1 - \frac{2}{3}\left(\frac{m}{\Lambda_2}\right)^2\left[\ln\left(\frac{\Lambda_2}{m}\right)^2 + \frac{1}{3}\right]\right) \tag{36}$$

This calculation is incorrect in that it does not modify the vertex so as to satisfy the Ward-Takahashi identity. McClure and Drell found that when they carried out the calculation so as to satisfy the Ward-Takahashi identity, they had two free cut off parometers, Λ_1 and Λ_2. They used for the vertex the expression

$$\bar{u}(p')\,\Gamma_\mu(p', p) = \bar{u}(p')\,\gamma_\mu\left[\left(\frac{m^2}{p^2 - m^2 - \Lambda_1^2}\right)\frac{p - m}{m} + \left(1 - \frac{p^2 - m^2}{p^2 - m^2 - \Lambda_2^2}\right)\right] \tag{37}$$

and found for the g-factor correction

$$\frac{g-2}{2} = \frac{\alpha}{2\pi}\left[1 + 2\left(\frac{m}{\Lambda_1}\right)^2 \ln\left(\frac{\Lambda_1}{m}\right)^2 - \frac{2}{3}\left(\frac{m}{\Lambda_2}\right)^2 \ln\left(\frac{\Lambda_2}{m}\right)^2\right] \tag{38}$$

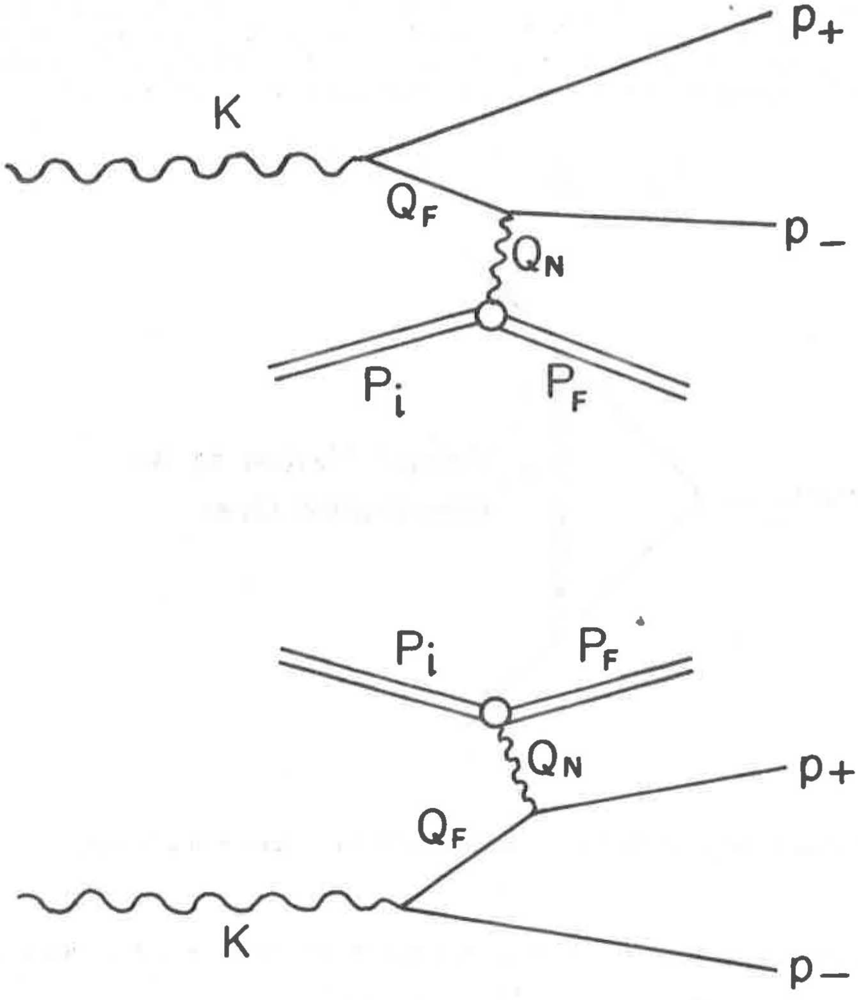

Figure 18 The Feynman diagrams for wide angle electron pair production.

Not only does this differ from equation 36 but in this case the fact that the expression is the difference of two logarithims makes it difficult to set definite limits on both cut off masses.

Another experiment which has been used as a test of quantum electrodynamics is the photoproduction of wide angle lepton pairs. The Feynman diagrams for wide angle pair production are shown in Figure 18. The cross section for this process is given by the Bethe-Heitler formula. In this process the virtual lepton is far off the mass shell so a measurement of the cross section tests the lepton propagator for large virtual space like momenta. The cross section calculated with the modified propagator of equation 35 is[53]

$$\sigma = \sigma_{BH} \left(\frac{1}{1 + \frac{p^2 - m^2}{\Lambda_2^2}} \right) \tag{39}$$

If the cross section is calculated with a modified propagator of equation 35 and the vertex is modified so as to satisfy the Ward-Takahashi identity, one obtains[53]

$$\sigma = \sigma_{BH} \left(1 + \frac{p^2 - m^2}{\Lambda_2^2} \right) \tag{40}$$

In one case the cross section increases as the four momentum of the virtual lepton increases; in the other case the cross section decreases as the four momentum of the virtual lepton increases. The chief moral to be gained from these calculations is that the measured cut off parameters should be regarded with suspicion. It is not clear just how the theory might be modified at small distances.

At present our best information on the behavoir of electrodynamics at high momenta comes from the correction to the g-factor of the muon, the comparison of electron-proton and muon-proton scattering, photoproduction of wide angle muon pairs, and photoproduction of wide angle electron pairs. There is also now available a preliminary result on electron-electron scattering from the Princeton-Stanford storage ring. The table summarizes the limits on the photon propagator, the muon vertex, and the muon propagation determined by the agreement of the measured muon g-factor with experiment[57]. These limits have been set using only simple modification such as equation 29 and they do not consider the Ward-Takahashi identity or the proper spectral form for the propagator or vertex functions. The manner in which the cut off mass enters the theoretical expression is such that the agreement between the electron g-factor and experiment can only be used to set weak limits on the photon propagator, the electron vertex, and the electron propagator.

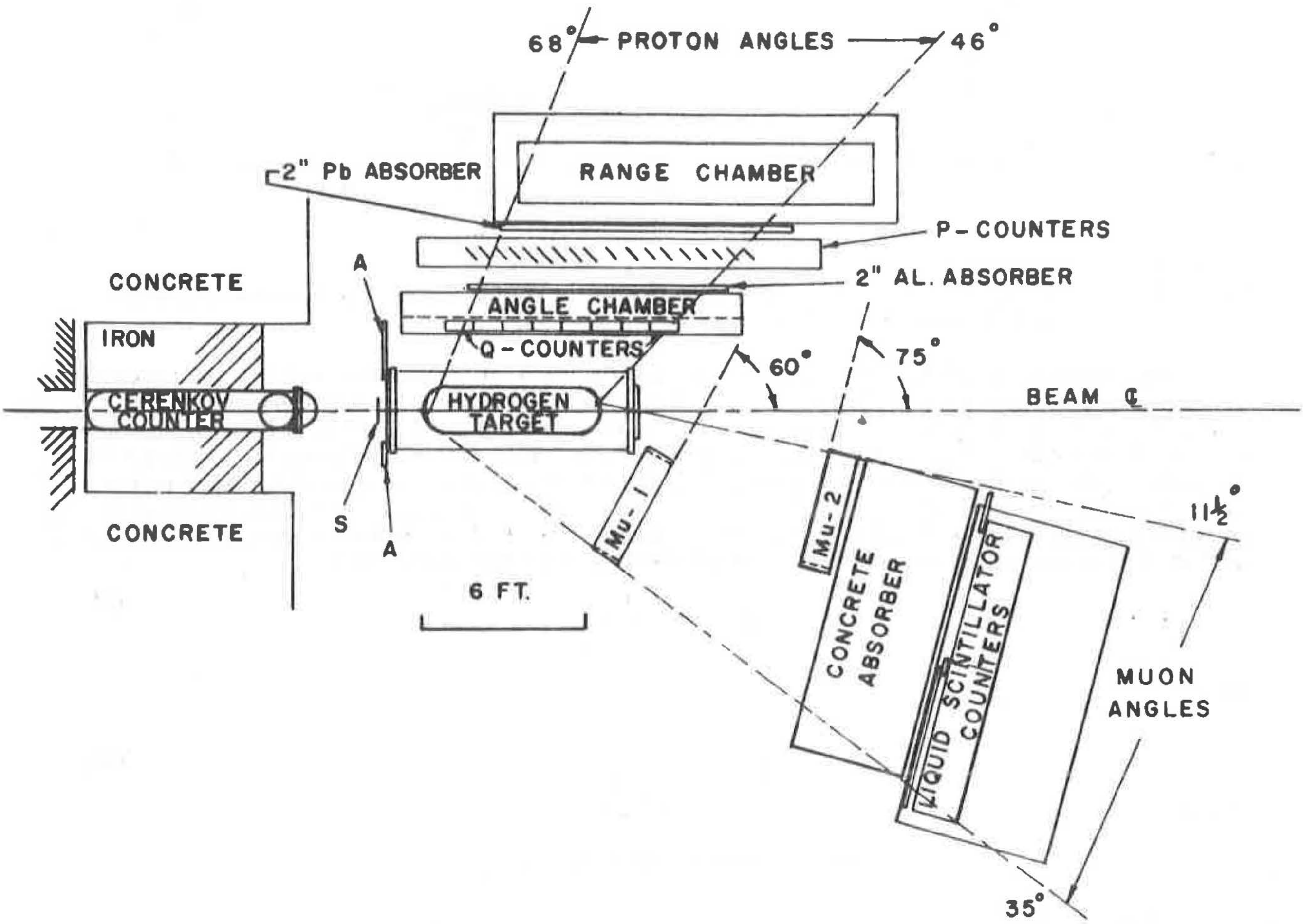

Figure 19 Experimental arrangement for the muon proton scattering. (From Cool et al, Ref. 58).

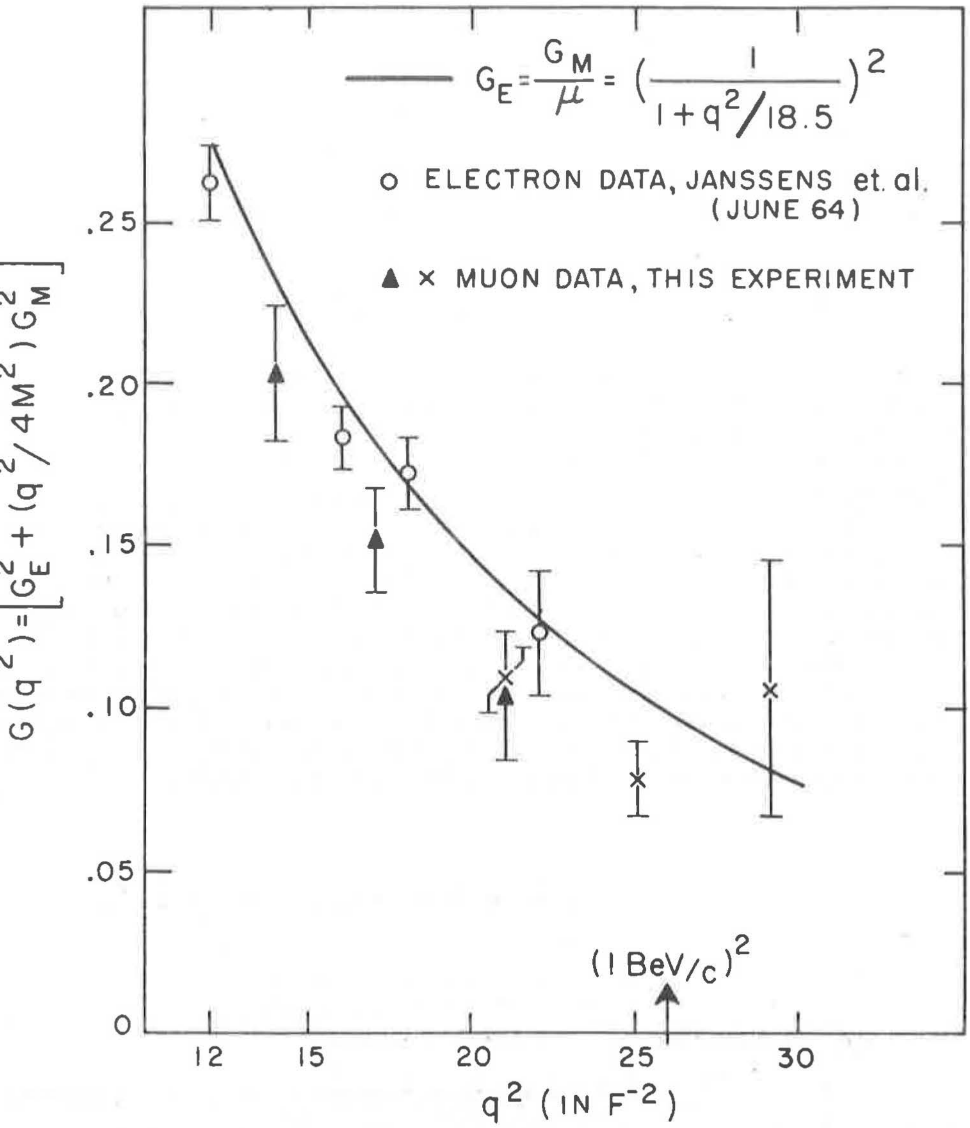

Figure 20 A comparison of the proton G factor as measured in muon-proton and electron-proton scattering. (From Cool et al, Ref. 58).

The most recent comparison of the muon-proton and the electron-proton scattering is the experiment by Cool et al at Brookhaven.[58] They used a spark chamber apparatus to measure muon-proton scattering in the q^2 range from 12 to 30 F^{-2}. Figure 19 shows a general outline of their apparatus. Figure 20 shows the comparison between the proton form factor determined from the muon-proton scattering experiment and the proton form factor determined by electron scattering experiments. The muon data has the same q^2 dependence as the electron scattering data but differs in absolute normalization by a factor of 1.18. The authors conclude that the form factor of the muon is the same as that of the electron. If the form factor of the leptons is written in the form

$$f(q^2) = \frac{1}{1 - \frac{q^2}{\Lambda^2}} \quad , \tag{41}$$

then

$$\frac{f_\mu}{f_e} = \frac{1}{1 - \frac{q^2}{D^2}} \quad , \tag{42}$$

where

$$|D^2| > 220\ F^{-2} \quad (2.9\ GeV/c) \ ,$$

with 95% confidence.

The most recent check on the muon propagator is the experiment of de Pagter et al at the Cambridge Electron Accelerator.[59] de Pagter et al measured the photo production from carbon of wide angle muon pairs. Figure 21 shows a general diagram of their apparatus. They used blocks of iron to

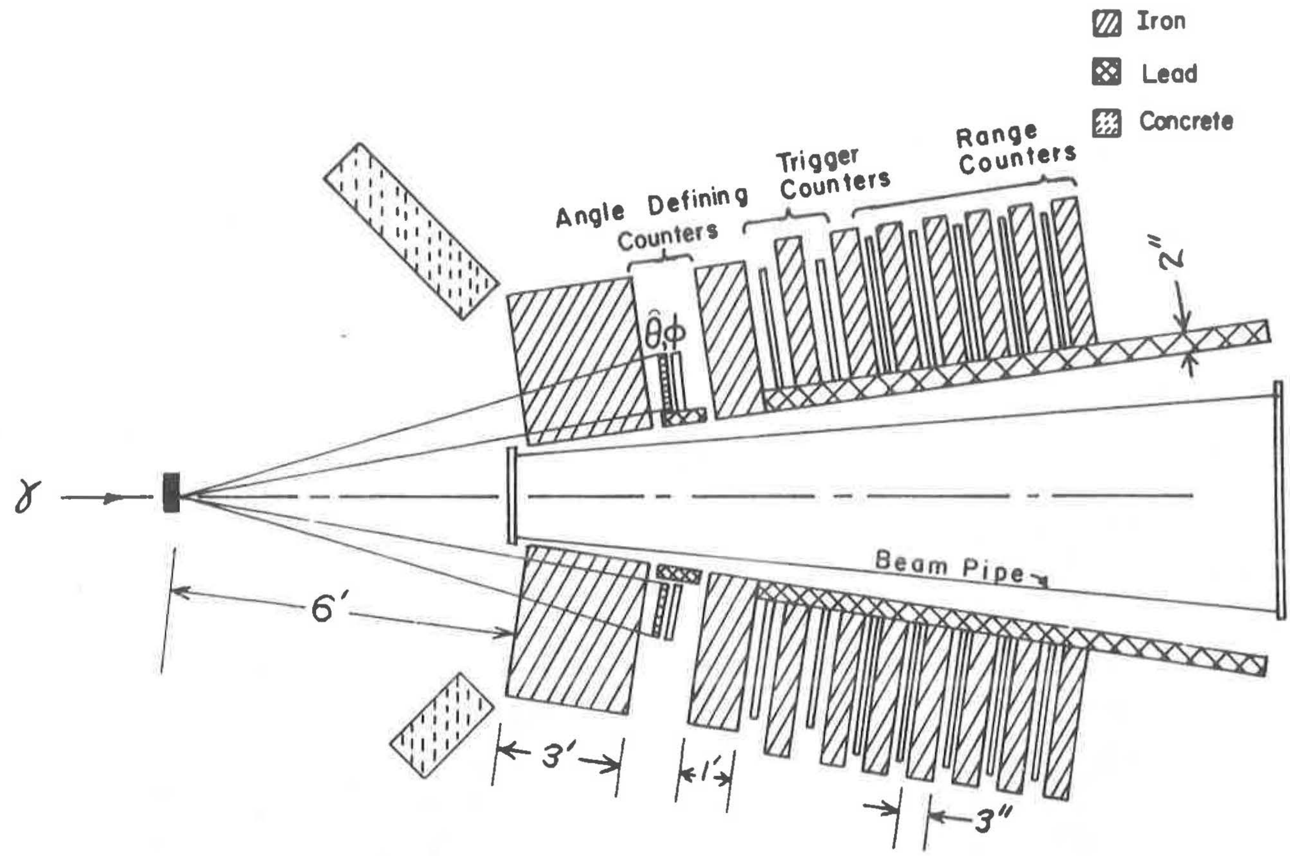

Figure 21 Schematic diagram of the apparatus for the study of the photo production of wide angle muon pairs from carbon. (From de Pagter et al, Ref. 59).

absorb the pions and a range counter system to determine the energy of the muons. They observed muons in the energy range from 1.8 to 2.4 GeV and in the range of polar angles from 4.5° to 11.5°. They then compared the yields for symmetrical pairs with the Monte Carlo calculation of the expected yields. Figure 22 shows a typical set of data together with the calculated cross section. de Pagter et al studied the dependence of the cross section for momenta of the virtual muon, q_F^2, between $1.3F^{-2}$ and $8F^{-2}$. They found for the ratio of theory to experiment for symmetrical pairs the expression was

$$R = \frac{\sigma_{exp}}{\sigma_{theo}} = (1.18 \pm 0.15) \; [1 - (0.11 \pm 0.021) \, |q_F^2| \,]$$

Using a breakdown model of the form

$$\frac{1}{q_F^2 - m_\mu^2} \longrightarrow \frac{1}{q_F^2 - m_\mu^2} - \frac{1}{q_M^2 - m_\mu^2 - \hbar\wedge_\mu^2}$$

they concluded that with 95% confidence

$$(\wedge_\mu)^2 > (6.2 \text{ F}^{-1})^2 = 38 \text{ F}^{-2} = (1.2 \text{ GeV}/c)^2 \; .$$

The most recent test of the electron propagator is the wide angle electron pair experiment of Blumenthal et al.[60] This experiment is quite interesting in that it indicates a deviation from the theory. The general apparatus used by Blumenthal et al is shown in Figure 23. They used two mirror image spectrometer systems to look at the electron pairs from a carbon target. Two quadrupole spectrometers were used to determine the momentum of the particles. A combination of Cerenkov and shower counters was used to separate the electrons from the pions. Blumenthal et al made measurements at electron momenta from 0.5 to 2.5 BeV/c and at pair half angles of 4.60, 6.23, and 7.50°. Figure 24 summarizes the measured points. A monte-Carlo integration was used to calculate the expected yields. Figure 25 shows the ratio of the experimental to theoretical yield as a function of the four momentum of the virtual electron and as a function of the energy of the outgoing electron-positron system. It is apparent from this figure that the experiment does not agree with theory.

There are two aspects of the disagreement. The yield is too small at low q^2 where electrodynamics has been well tested and the yield has the wrong behavior as a function of energy. The failure of experiment to agree with theory at low q^2 can be explained as an error in the absolute normalization. Both of these problems were investigated by a study of the single channel electron rates. The single channel electrons came from relatively well understood low momentum transfer processes so one

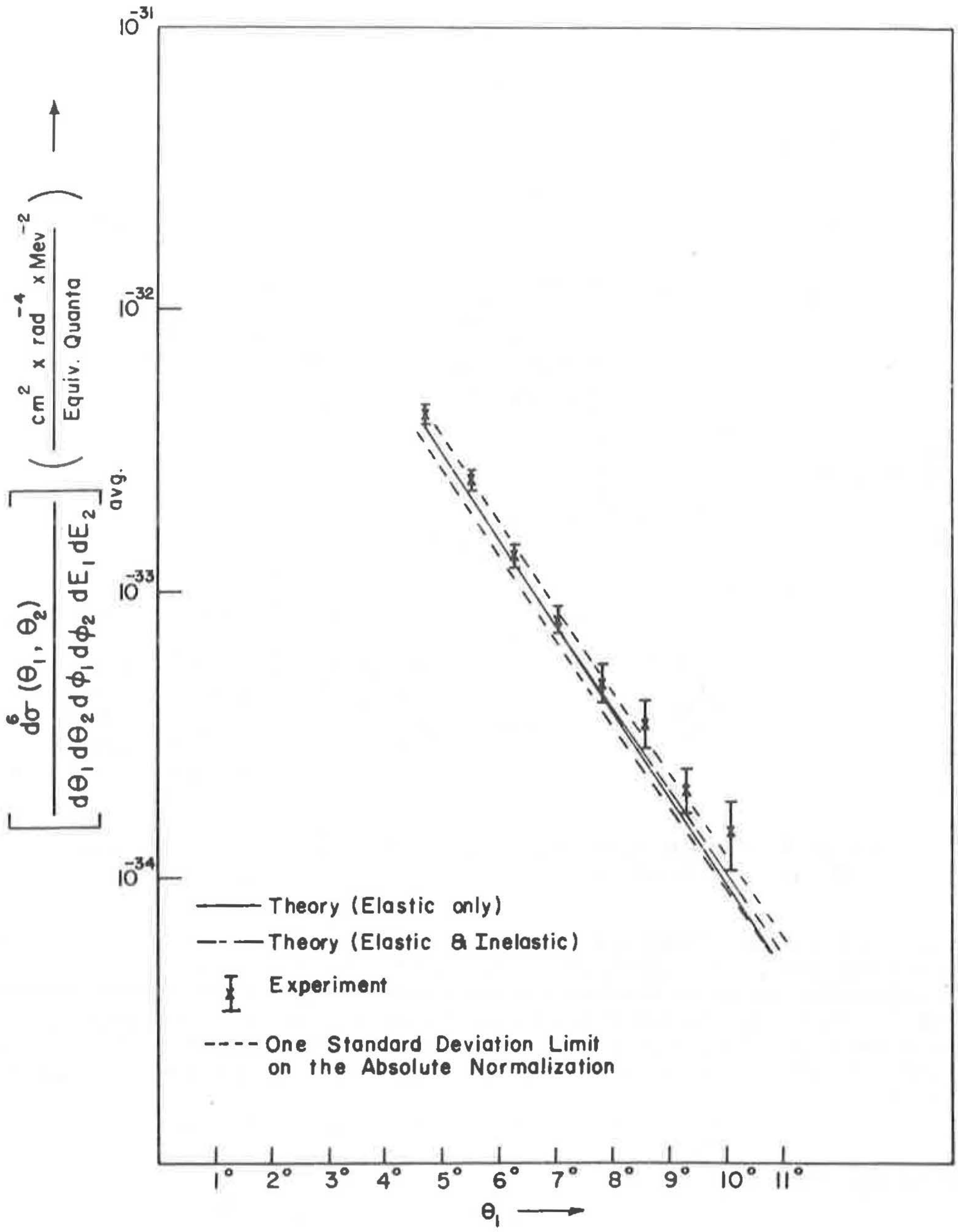

Figure 22 A comparison between the measured cross section for wide angle muon pairs and the theoretical cross section. (From de Pagter et al, Ref. 59).

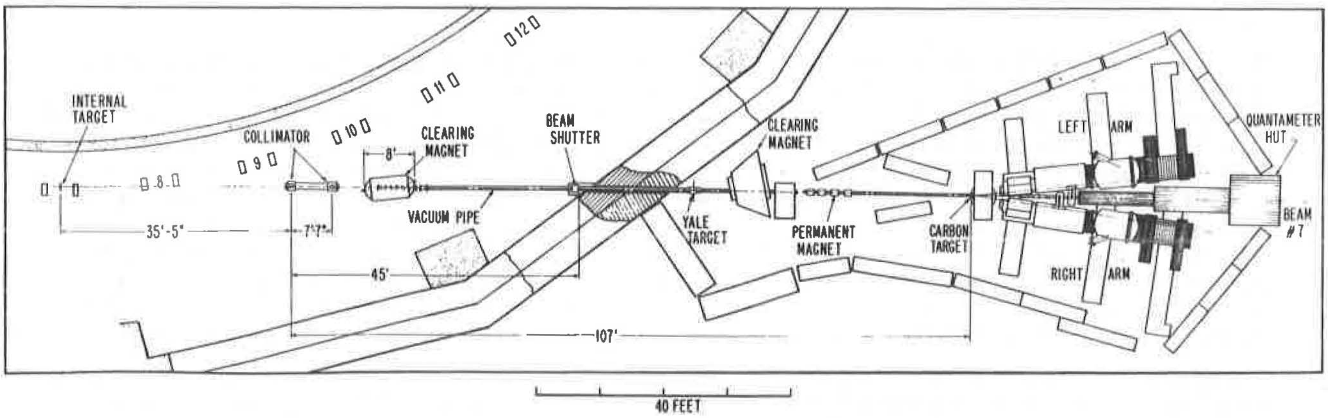

Figure 23 The schematic diagram of the apparatus used in the wide angle electron pair experiment. (From Blumenthal et al, Ref. 60).

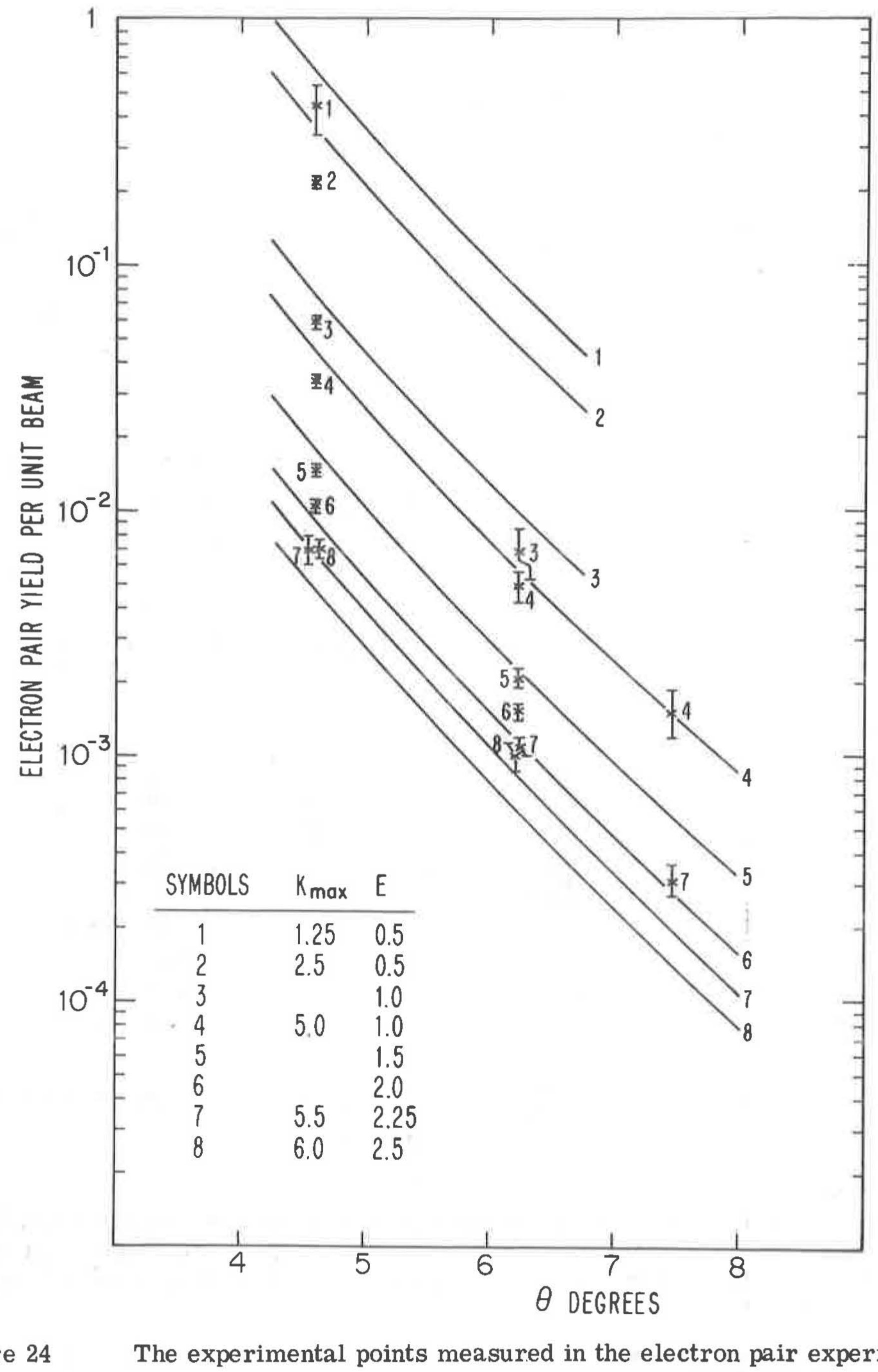

Figure 24 The experimental points measured in the electron pair experiment.

does not expect the experimental yields to deviate from theory. There are two sources of single channel electrons - direct pair production such that one member of the pair is produced at a wide angle and forward pair production followed by a scattering in the target of one of the electrons into the aperature. The yield for the first process increases as the target thickness; the yield for the second processes increases as the target thickness squared. Figure 26 shows a comparison between the experimental and theoretical yields for each of the four channels. This data suggests that the phase space acceptance of each channel was somewhat different than it was calculated to be but that to 10% or 15% the acceptance was the expected function of momentum. Thus Figure 26 suggests that the error in the electron pair experiment is one of absolute normalization and that the deviation of the energy dependence from theory is real. Another way to show this is form the ratio

$$R_M = \frac{R_{pairs}}{R_{leftarm}\ R_{rightarm}}$$

That is the ratio of theory to experiment for electron pairs is divided by the product of the ratios of theory to experiment for the left arm single channel rates and the right arm single channel rates. This normalizes the pair data to the single channel data. Figure 27 shows a plot of this ratio for the t and t^2 single channel rates. This figure indicates that the deviation of experiment from theory is real.

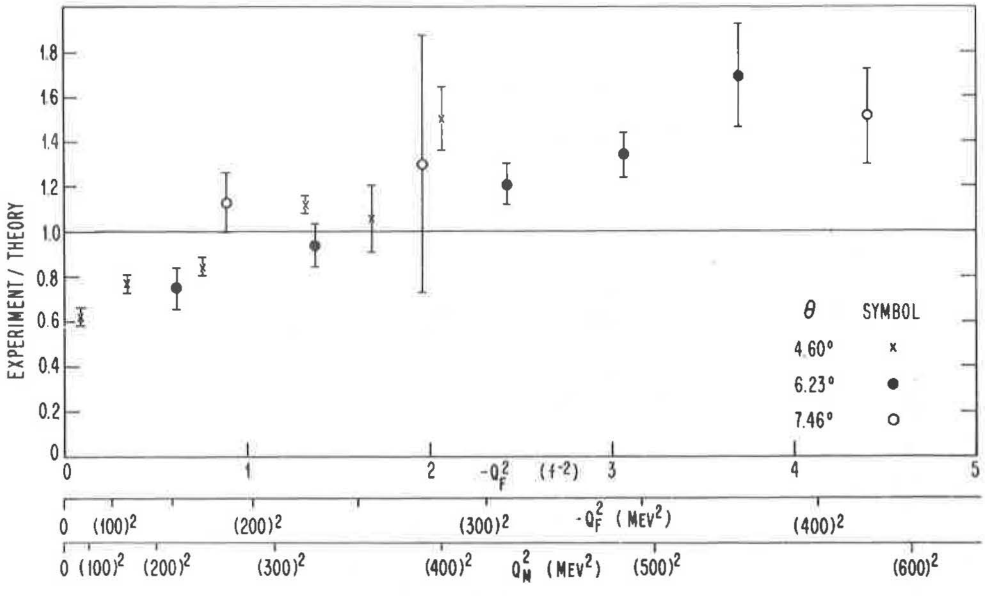

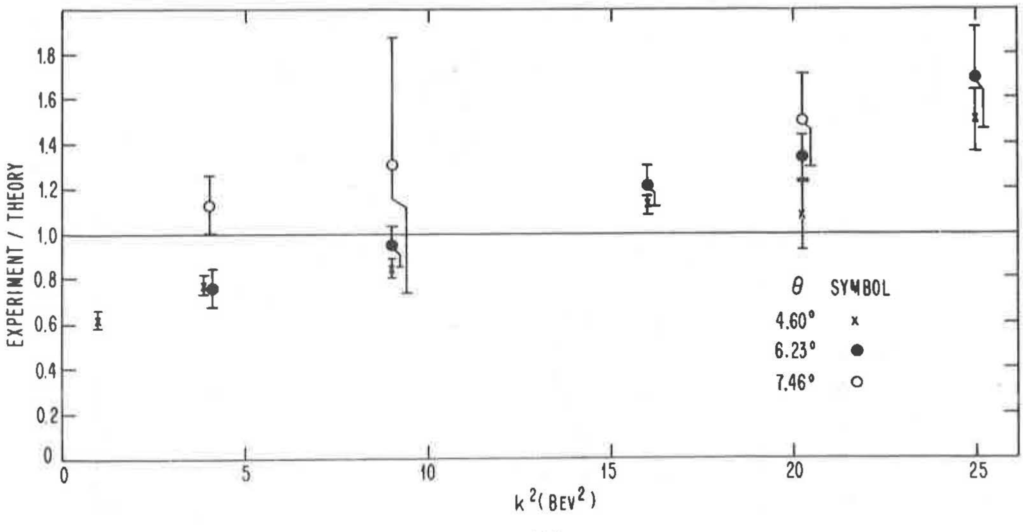

Figure 25 Plots showing the ratio, R, of theory to experiment for the wide angle electron pairs. Part (a) shows the ratio as a function of the four momentum of the virtual lepton; part (b) shows the ratio as a function of the energy of the outgoing electron-positron system.

One can ask whether the deviation from theory found in the electron pair experiment is due to a breakdown of electrodynamics or to the presence of some other process. Another source of electrons is the Compton diagrams shown in Figure 28. Estimates by Drell based on a dispersion theory calculation of forward Compton scattering followed by pair production and of electron pairs from rho decay using the measured rates of rho production indicate that the Compton correction is less than a few percent.[61] Low has suggested that the deviation could be due to a heavy electron which decays into an ordinary electron and a photon.[62] Unsuccessful searches for such a particle have been made at Orsay and the Cambridge Electron Accerlator.[63,64,65] At this conference Behrend et al[66] reported a new search for an excited electron in the mass range from 0.5 to 1.1 GeV. They used a coincidence apparatus consisting of two quadrupole spectrometers. The electron angle was fixed at 32° in the laboratory system and the mass of the e* was varied by changing the angle of the proton spectrometer. If the e*-e coupling is expressed in the form

$$\lambda \frac{e}{M^*} \sigma_{\mu\nu} F^{\mu\nu}$$

then their result shows that $\lambda = \frac{1}{70}$ with 95% confidence.

At this conference Richter[67] reported on the first results from the Princeton-Stanford storage rings. The storage rings are now working and they have measured the angular distribution of elastic electron-electron scattering at a total energy of 600 MeV in the centre-of-mass system and over the angular range from 40° to 90°. They have compared the measured angular distribution of 416 events to the

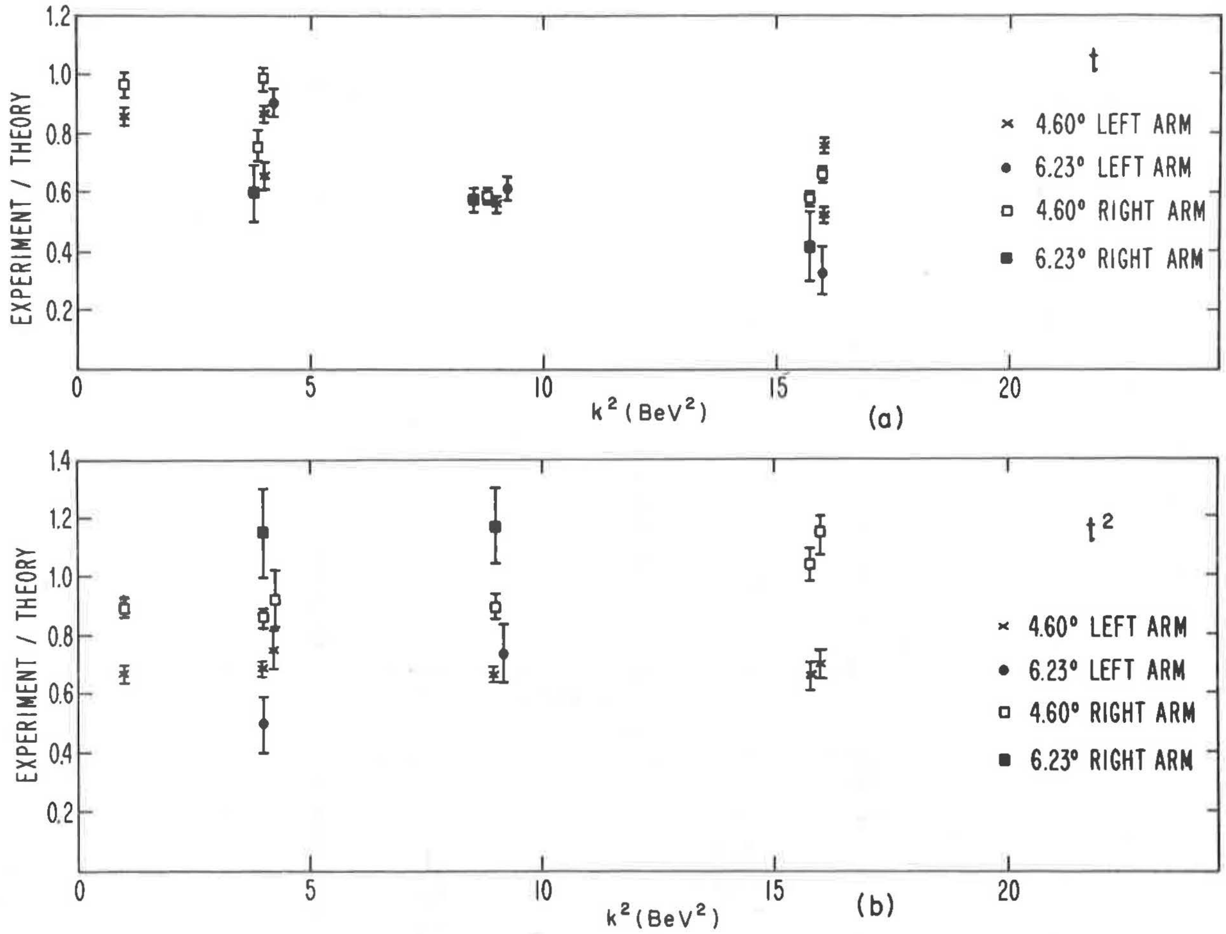

(b)

Figure 26 A plot showing the ratio of theory to experiment for the singe channel electron rates. Part (a) shows the comparison for that part of the rate which increases as the target thickness; part (b) shows the comparison for that part of the rate which increases as the target thickness squared.

Møller cross section with a form factor added. The two Feynman diagrams for electron-electron scattering are shown in Figure 29. The momentum transfer is unique only at 90°; at other angles it is different for the direct scattering and the exchange scattering. The cross section for electron-electron scattering is

$$\frac{d\sigma}{d\Omega} = \frac{\pi\alpha^2}{4E^2}\left\{\frac{4+(1+\cos\varphi)^2}{(1-\cos\varphi)^2}\,|F(q^2)|^2 + \frac{8}{\sin^2\varphi}\,\mathrm{Re}[F^*(q^2)F(q'^2)] + \frac{4+(1-\cos\varphi)^2}{(1+\cos\varphi)^2}\,|F(q'^2)|\right\},$$

where

$$q^2 = 4E^2\sin^2\varphi/2$$
$$q'^2 = 4E^2\cos^2\varphi/2$$

They analyzed these results by using a form factor of the form

$$F(q^2) = \frac{1}{1 - q^2/\Lambda^2}$$

and adjusting Λ so as to fit the data. For each value of Λ the angular distribution was normalized so as to fit the χ^2. On this basis they found that

$0.77\ \mathrm{GeV}/c \leqslant \Lambda \leqslant \infty$ 68% confidence and

$\Lambda \geqslant 0.55\ \mathrm{GeV}/c$ (Λ^2 positive)
$\Lambda \geqslant 0.98\ \mathrm{GeV}/c$ (Λ^2 negative) 99% confidence

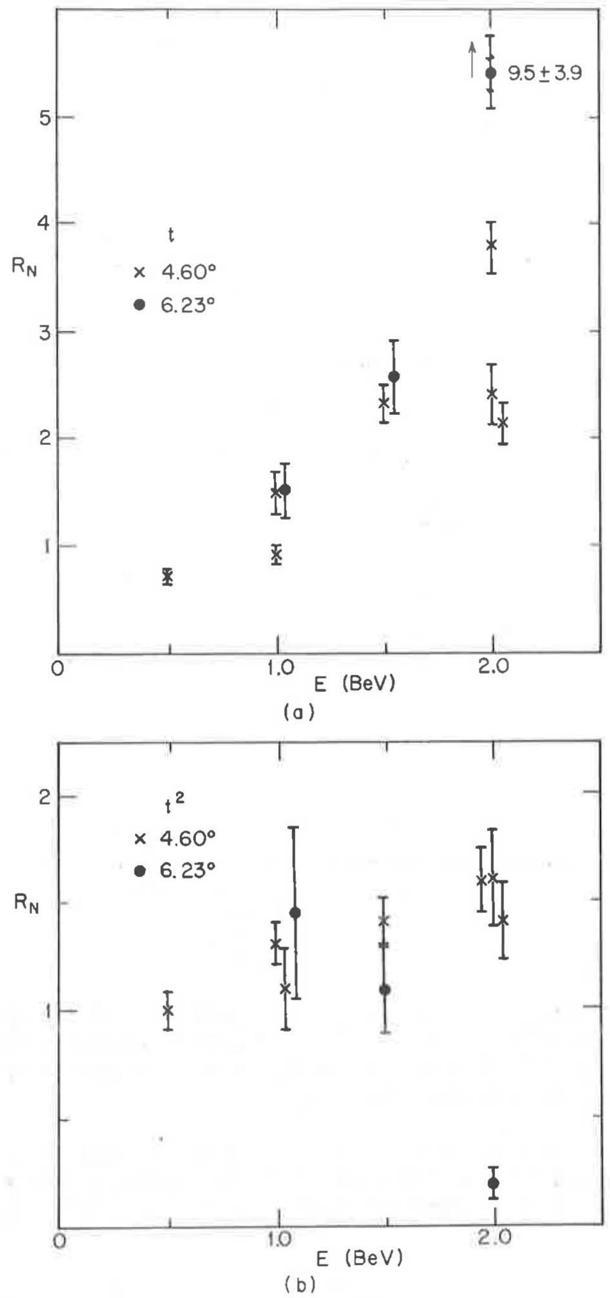

Figure 27 The ratio of theory to experiment for the electron pair experiment normalized to the product of the ratios of theory to experiment for the left and right arms.

Table

A summary of the lower limits of the cutoff parameter for the photon propagator, the muon vertex, and muon propagator determined from the agreement between theory and experiment of the g-factor of the muon. This limit corresponds to the 68% confidence level. From F.J.M. Farley, Progress in Nuclear Physics (Pergamon Press, Oxford), vol. 9, 255 (1964).

	(GeV/c)	Distance in F
Photon propagator	1	0.2
Muon vertex	1.3	0.15
Muon propagator	2.7	0.07

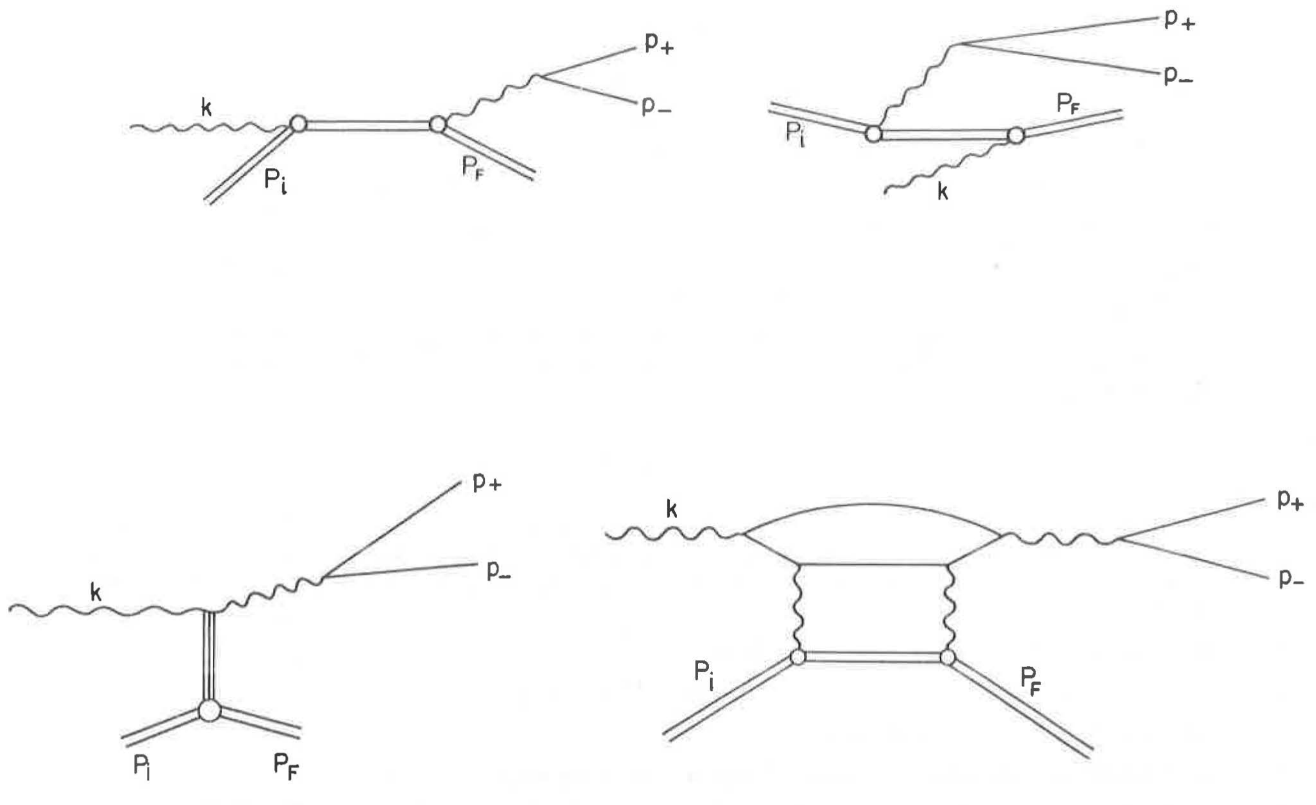

Figure 28 Feynman diagrams for Compton processes which can give rise to wide angle electron pairs.

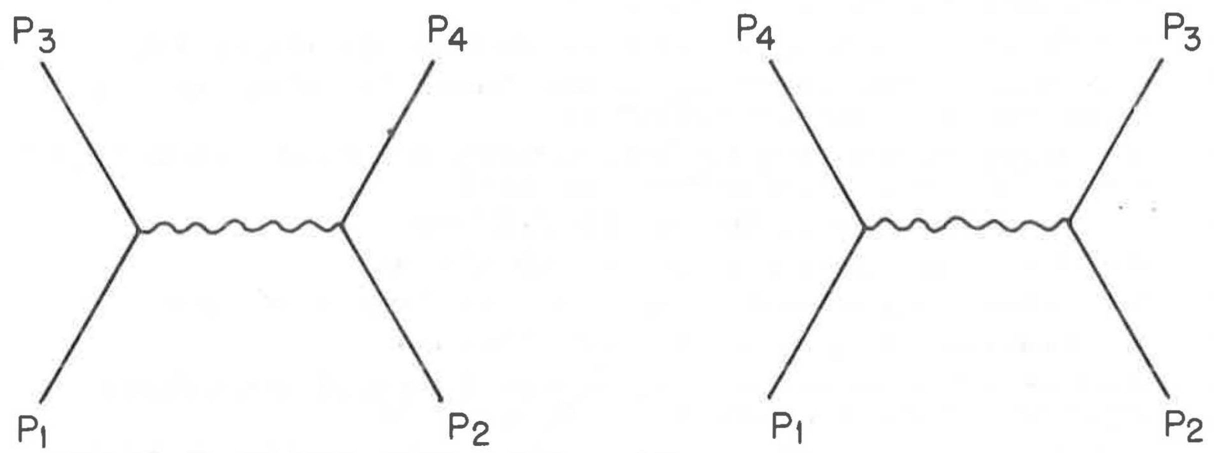

Figure 29 Feynman diagrams for electron-electron scattering.

References

1. Some recent review articles or books on the general subject of electron scattering are the following:

   (a) S.D. Drell and F. Zachariasen, Electromagnetic Structure of Nucleons (Oxford, 1961).

   (b) R. Hofstadter, Ed., Nuclear and Nucleon Structure (Benjamin, New York, 1963).

   (c) L.N. Hand, D.G. Miller, and R. Wilson, Rev. Mod. Phys. **35**, 335 (1963).

   (d) R.R. Wilson and J.S. Levinger, Annual Reviews of Nuclear Science (Annual Reviews, Inc., Palo Alto, Calif. 1964), **14**, p. 135.

2. It is conventional in papers on electron scattering to choose a metric such that the momentum transfer in electron scattering is positive. We shall not follow this convention but instead use the metric

$$p^2 = (p_0^2 - \vec{p} \cdot \vec{p})$$

   For this metric the momentum transfer in electron scattering is negative. It is also conventional in the electron scattering literature to measure the momentum transfer in inverse fermis (F^{-1}). The conversion to MeV/c can be made by noting that $1F^{-1}$ corresponds to 197 MeV/c.

3. R.G. Sachs, Phys, Rev. **126**, 2256 (1962).
4. V. Barger and R. Carhart, Phys. Rev. **136**, B281 (1964).
5. M. Gourdin and A. Martin, preprint (CERN).
6. D. Flamm and W. Kummer, Nuovo Cimento **28**, 33 (1963).
7. J.R. Dunning, Jr., K.W. Chen, N.F. Ramsey, J.R. Rees, W. Shlaer, J.K. Walker, and Richard Wilson, Phys. Rev. Letters **10**, 500 (1963).
8. K. Berkelman, M. Feldman, and G. Rouse, Phys. Letters **6**, 116 (1963).
9. A. Browman, F. Liu, and C. Schaerf, Phys. Rev. **139**, B1079 (1965).
10. D. Yount and J. Pine, Phys. Rev. **128**, 1842 (1962).
11. J.C. Bizot, J.M. Buon, J. LeFrancois, J. Perez y Jorba, and Ph. Roy, Phys. Rev. Letters **11**, 480 (1963).
12. S.D. Drell and M.A. Ruderman, Phys. Rev. **106**, 561 (1957).
13. S.D. Drell and S. Fubini, Phys. Rev. **113**, 741 (1959).
14. F. Guérin and C.A. Piketty, Proceedings of the Sienna International Conference on Elementary Particles, Vol. I, p. 371.
15. E.B. Hughes, T.A. Griffy, M.R. Yearian, and R. Hofstadter, Phys. Rev. **139**, B458 (1965).
16. L.H. Chan, K.W. Chen, J.R. Dunning, Jr., N.F. Ramsey, J.K. Walker, and Richard Wilson, Phys. Rev. (submitted for publication).
17. K.J. Barnes, P. Carruthers, and F. von Hipple, Phys. Rev. Letters **14**, 82 (1965).
18. K.W. Chen, A.A. Cone, J.R. Dunning, Jr., N.F. Ramsey, J.K. Walker, and Richard Wilson, Phys. Rev. (submitted for publication).
19. J.R. Dunning, Jr., K.W. Chen, A.A. Cone, G. Hartwig, N.F. Ramsey, J.K. Walker, and Richard Wilson, Phys. Rev. (submitted for publication).
20. S.M. Berman and S.D. Drell, Phys. Rev. **133**, B791 (1964).
21. M. Gell-Mann and F. Zachariasen, Phys. Rev. **124**, 953 (1961).
22. M. Gell-Mann, R. Sharp, and W.G. Wagner, Phys. Rev. Letters **8**, 261 (1962).
23. R.F. Dashen and D.H. Sharp, Phys. Rev. **133**, B1585 (1964).
24. For a general discussion and relevant references see G. Källen, Elementary Particle Physics (Addison-Wesley, Reading, Mass.) 1964, pp. 230-234.
25. D.J. Hughes, J.A. Harvey, M.D. Goldberg, and M.J. Stafne, Phys. Rev. **90**, 497 (1953).
26. E. Melkonian, B.M. Rustad, and W.W. Havens, Jr. Phys. Rev. **114**, 1571 (1959).
27. O. Halpern, Phys. Rev. **133**, B579 (1964).
28. T. Janssens, E.B. Hughes, M.R. Yearian, and R. Hofstadter (to be published).
29. A. Zichichi, S.M. Berman, N. Cabibbo, and R. Gatto, Nuovo Cimento **24**, 170 (1962).

30. For a general treatment of quantum electrodynamics see for example S.S. Schweber, An Introduction to Relativistic Quantum Field Theory (Row-Peterson and Co., Evanston, Illinois, 1961).

31. A.J. Layzer, J. Math. Physics **2**, 306 (1961).

32. G.W. Erickson (to be published).

33. S. Triebwasser, E.S. Dayhoff, and W.E. Lamb, Jr., Phys. Rev. **89**, 98 (1953).

34. R.T. Robiscoe, Phys. Rev. **138**, A22 (1965).

35. G.W. Erickson, Phys. Rev. Letters **15**, 338 (1965).

36. C.Y. Fan, M. Garcia-Munoz, and I.A. Sellin, Phys. Rev. Letters **15**, 15 (1965).

37. C.M. Sommerfield, Phys. Rev. **107**, 328 (1957); Ann. Phys. (N.Y.) **5**, 26 (1958).

38. A. Petermann, Helv. Phys. Acta. **30**, 407 (1957).

39. S.D. Drell and H.R. Pagels (Phys. Rev. -- to be published).

40. D.T. Wilkinson and H.R. Crane, Phys. Rev. **130**, 852 (1963).

41. E.S. Dayhoff, S. Triebwasser, and W.E. Lamb, Jr., Phys. Rev. **89**, 106 (1953).

42. H.A. Bethe and E.E. Saltpeter, Quantum Mechanics of One and Two-Electron Atoms (Academic Press, Inc., New York, N.Y. 1957), 1st ed., p. 352.

43. H. Suura and E.H. Wichmann, Phys. Rev. **105**, 1930 (1957).

44. A. Petermann, Phys. Rev. **105**, 1931 (1957).

45. G. Charpak, F.J.M. Farley, R.L. Garwin, T. Muller, J.C. Sens, and A. Zichichi, Physics Letters **1**, 16 (1962).

46. R. Karplus and A. Klein, Phys. Rev. **86**, 257 (1952).

47. R. Weinstein, M. Deutsch, and S. Brown, Phys. Rev. **98**, 223 (1955).

48. W.E. Cleland, J.M. Bailey, M. Eckhause, V.W. Hughes, R.M. Mobley, R. Prepost, and J.E. Rothberg, Phys. Rev. Letters **13**, 202 (1964).

49. C.K. Iddings, Phys. Rev. **138**, B446 (1965).

50. S.D. Drell, Ann. Phys. **4**, 75 (1958).

51. B. de Tollis, Nuovo Cimento **16**, 203 (1960).

52. V.B. Berestetsky, JEPT **12**, 993 (1961).

53. J.A. McClure and S.D. Drell, Nuovo Cimento (to be published).

54. G. Källen, Helv. Phys. Acta. **25**, 417 (1952).

55. J.C. Ward, Phys. Rev. **77**, 293 (1950).

56. Y. Takahashi, Nuovo Cimento **6**, 371 (1957).

57. F.J.M. Farley, Progress in Nuclear Physics (Pergamon Press, Oxford), Vol. 9, p. 255.

58. R. Cool, A. Maschke, L.M. Lederman, M. Tannenbaum, R. Ellsworth, A. Melissinos, J.H. Tinlot, and T. Yamanouchi, Phys. Rev. Letters **14**, 724 (1965).

59. J.K. de Pagter, A. Boyarski, G. Glass, J.I. Friedman, H.W. Kendall, M. Gettner, J.F. Larrabee, and Roy Weinstein, Phys. Rev. Letters **12**, 739 (1964).

60. R.B. Blumenthal, D.C. Ehn, W.L. Faissler, P.M. Joseph, L.J. Lanzerotti, F.M. Pipkin, and D.G. Stairs, Phys. Rev. Letters **14**, 660 (1965).

61. S.D. Drell, Invited paper at Hamburg International Conference on Electron and Photon Interactions, June 1965.

62. F.E. Low, Phys. Rev. Letters **14**, 238 (1965).

63. C. Betourne, H. Nguyen Ngoc, J. Perez y Jorba, and J. Tran Thanh Van, Physics Letters **17**, 70 (1965).

64. R. Wilson (private communication).

65. J. Friedman (private communication).

66. H.J. Behrend, F.W. Brasse, J. Engler, E. Ganssauge, H. Hultschig, S. Galster, G. Hartwig, and H. Schopper, Report to Oxford International Conference on Elementary Particles, Sept. 19-25 1965 (Unpublished).

67. W.C. Barber, B. Richter, B. Gittlemar, and G.K. O'Neill, Report to Oxford International Conference on Elementary Particles, Sept. 19-25 1965 (Unpublished).